



Prediction of Flashover Voltage of Insulators Using Low Voltage Surface Resistance Measurement

Final Project Report

Power Systems Engineering Research Center

*A National Science Foundation
Industry/University Cooperative Research Center
since 1996*





Power Systems Engineering Research Center

Prediction of Flashover Voltage of Insulators Using Low Voltage Surface Resistance Measurement

Final Project Report

Project Team

**Ravi S. Gorur, Project Leader, Arizona State University
Robert Olsen, Washington State University**

Industry Advisors

**Jim Crane and Tom Adams, Exelon
Jim Gurney and Jim Duxbury,
British Columbia Transmission Corp.**

Graduate Student

Sreeram Venkataraman, Arizona State University

PSERC Publication 06-42

November 2006

Information about this project

For information about this project contact:

Ravi S. Gorur, Ph.D.
Professor of Electrical Engineering
Arizona State University
Tempe, AZ 85287-5706
Phone: 480-965-4894
Fax: 480-965-0745
Email: ravi.gorur@asu.edu

Power Systems Engineering Research Center

This is a project report from the Power Systems Engineering Research Center (PSERC). PSERC is a multi-university Center conducting research on challenges facing a restructuring electric power industry and educating the next generation of power engineers. More information about PSERC can be found at the Center's website: <http://www.pserc.org>.

For additional information, contact:

Power Systems Engineering Research Center
Arizona State University
577 Engineering Research Center
Box 878606
Tempe, AZ 85287-8606
Phone: 480-965-1643
FAX: 480-965-0745

Notice Concerning Copyright Material

PSERC members are given permission to copy without fee all or part of this publication for internal use if appropriate attribution is given to this document as the source material. This report is available for downloading from the PSERC website.

© 2006 Arizona State University. All rights reserved.

ACKNOWLEDGEMENTS

This is the final report for the Power Systems Engineering Research Center (PSERC) research project titled “Prediction of Flashover Voltage of Insulators Using Low Voltage Surface Resistance Measurement” (PSERC T-26G). We express our appreciation for the support provided by PSERC’s industrial members and by the National Science Foundation under grant NSF EEC-0001880 received from the Industry / University Cooperative Research Center program.

We also express our appreciation for the special financial support provided by PSERC’s industrial members, Exelon and British Columbia Transmission Corp (BCTC). Technical guidance from Mr. Jim Crane and Mr. Tom Adams, Exelon; and Mr. Jim Gurney and Mr. Jim Duxbury of BCTC is appreciated.

EXECUTIVE SUMMARY

Failures of high voltage insulators on transmission lines can lead to transmission line outages, thereby reducing system reliability. One form of insulator failure is flashover, the unintended disruptive electric discharge over or around the insulator. Contamination on the surface of the insulators, such as from salts for de-icing streets and sidewalks, enhances the chances of flashover. Currently there are no standardized tests for understanding the contamination flashover performance of polymeric insulators. This research project developed models by which the flashover voltage can be predicted and flashover dynamics explained for contaminated polymeric insulators. The model developed can be applied to contaminants such as sea salt, road salt, and industrial pollution found in many locations. The results from this work are useful for selecting the appropriate insulator design (including dimensions and material) for different system voltages. This work finds applications in distribution class insulators and can be extended to higher voltage classes.

The principle dielectrics used for outdoor insulators are ceramics and polymers. In early high voltage transmission and distribution system designs, ceramic insulators made of porcelain or glass were used principally. Since the 1960's, however, polymers have been preferred for the housing of high voltage outdoor materials. In the last twenty-five years, the use of polymeric materials, particularly silicone rubber and ethylene propylene diene monomer, as weathersheds on outdoor insulators has increased substantially.

Polymers have low values of surface energy. This forces the polymeric materials to inhibit the formation of continuous water film and causes the formation of only isolated water droplets. Thus, polymers repel water (that is they are hydrophobic) and limit leakage current much better than porcelain. Hence, they are less susceptible to contamination-based flashovers than porcelain insulators.

Contamination on outdoor insulators enhances the chances of flashover. Under dry conditions, contaminated surfaces do not conduct so contamination is of little concern. Under environmental conditions of light rain, fog or dew, surface contamination dissolves. This promotes a conducting layer on an insulator's surface which facilitates a leakage current. High current density near the electrodes results in the heating and drying of the pollution layer. An arc is initiated if the voltage stress across the insulator's dry band exceeds its withstand capability. Extension of the arc across the insulator ultimately results in flashover. The contamination severity determines the frequency and intensity of arcing and, thus, the probability of flashover.

In practice, there are various contaminant types that settle on outdoor insulators. These contaminants can be classified as soluble and insoluble. Insulators located near coastal regions are typically contaminated by soluble contaminants, especially salt (or sodium chloride). Insulators located near cement or paper industries are typically contaminated by non-soluble contaminants such as calcium chloride, carbon and cement dust. Irrespective of the type of contaminant, flashover can occur as long as the salts in the contaminant are soluble enough to form a conducting layer on the insulator's surface.

Salts used for de-icing streets, roads and sidewalks include sodium chloride, calcium chloride, potassium chloride, calcium magnesium acetate, and magnesium chloride. Of these chemical compounds, the most commonly used road salts are sodium chloride and calcium chloride. After application, these road salts tend to be deposited on insulator surfaces by the effects of atmospheric wind and vehicle movement. The effect these road salts have on insulators depends on the physical state in their application to the road. Deicing streets with a liquid form

of salt is a new practice and is expected to have the worst effect on insulator performance.

Due to the hydrophobic nature of non-ceramic insulators, the best flashover prediction method may not be measurement of the amount of salt contaminate on the insulator's surface. A hydrophobic surface can have high contaminate levels with negligible leakage current because water formation on such a surface is in the form of discrete droplets as opposed to a continuous film. An alternate method for predicting the flashover voltage studied in this research is the measurement of surface resistance under wet conditions. To date there has not been much work done in characterizing the surface resistance values that would be indicative of either flashover or withstand. The type of fog and rate of wetting of the insulators also affects the surface resistance of non-ceramic insulators. It is easier to measure the contamination level than the surface resistance. Thus, there is a need to determine the correlation between the two measurements. The guidelines are well defined for surface resistance measurements in laboratories under various test conditions.

A combination of theoretical modeling, experiments and regression analysis was used to evaluate the flashover performance of outdoor insulators under contaminated conditions. The theoretical part consisted of developing a model to predict flashover voltage of ceramic and non-ceramic insulators. The model was based on reignition and arc constants derived from electric field calculations, and surface resistance of polluted insulators determined using experiments in a laboratory. Experiments were performed on distribution class insulators employing porcelain, silicone rubber and ethylene propylene diene monomer (EPDM) rubber as housing materials. It was shown that using surface resistance values measured at relatively low voltages, it is possible to assess insulator performance including such important factors as hydrophobicity, aging, and contamination accumulation.

A wide-range of analyses can be conducted with the approach developed in the study. Here are some findings from the research.

- For EPDM non-ceramic insulators, a critical value was determined of surface resistance that will result in a flashover. This information is useful for assessing the condition of similar non-ceramic insulators in use.
- The experiments and simulations on road salts indicated that the application of liquid salts has an immediate deleterious effect on insulator performance and will enhance flashover more severely than other salts.
- In any shed, the increase in number of water droplets shows an increase in electric field at the tip of the shed. As we move away from the high voltage end, the increase in electric field value at the water droplet - shed junction is significantly lower than observed for the shed that is closest to high voltage end.
- For the same level of contamination (as measured by Equivalent Salt Deposit Density or ESDD), the flashover voltage for an aged silicone rubber is about 12% less than new silicone rubber. Aged EPDM has a flashover voltage that is about 16% lower than aged silicone rubber, and porcelain has a flashover voltage that is about 16% lower than aged EPDM.
- The superior performance of aged silicone material over EPDM was quantified.

An important next step in this line of research is the development of a low voltage tool for measuring surface resistance. That this is the next step resulted from this research demonstrating the validity of assessing insulator performance by measuring surface resistance for ceramic and non-ceramic insulators.

TABLE OF CONTENTS

| | | |
|---|---|----|
| 1. | Introduction | 1 |
| 1.1 | Overview | 1 |
| 1.2 | Contamination Flashover | 2 |
| 1.3 | Nature of Contaminants..... | 3 |
| 1.4 | Importance of Surface Resistance Measurement (NCI)..... | 4 |
| 1.5 | Need for Work in Flashover Prediction (Especially for NCI)..... | 5 |
| 2. | Flashover Theory, Evaluation and Measurement of Contamination..... | 6 |
| 2.1 | Flashover Mechanisms - General Theory and Obenaus Model | 6 |
| 2.2 | Flashover Theory of Various Other Researchers | 7 |
| 2.3 | Flashover Theory in Partially Contaminated Insulators..... | 8 |
| 2.4 | Measurement of Contamination Severity..... | 9 |
| 2.5 | Evaluation of Contamination Flashover Performance in Laboratories | 9 |
| 2.6 | Surface Resistance for Characterizing Flashover..... | 10 |
| 3. | Experimental Set up | 12 |
| 3.1 | Fog Chamber Description | 12 |
| 3.2 | Artificial Contamination of Non Ceramic Insulators | 12 |
| 3.3 | Measurement of Surface Conductivity and Calculation of ESDD..... | 13 |
| 3.4 | Testing Procedure for Surface Resistance Measurement and Estimation of FOV..... | 14 |
| 4. | Results and Analysis | 15 |
| 4.1 | Comparison of Simulated Results of Various Arc Models | 15 |
| 4.2 | Analysis of Test Results of Different Road Salts..... | 17 |
| 4.3 | Effect of Water Droplets in Different Sheds | 21 |
| 4.4 | Development of a Model to Predict FOV Based on ESDD Variation for Non-Ceramic and Ceramic Insulators | 22 |
| 4.5 | Development of a Model to Predict FOV Based on Surface Resistance Measurement for Non-Ceramic Insulators..... | 30 |
| 4.6 | Development of a Model to Predict FOV Based on Leakage Distance | 38 |
| 4.7 | Study of Recovery Aspects of Silicone Rubber and EPDM via Surface Resistance Measurements..... | 42 |
| 4.8 | Theoretical Model for NCI..... | 45 |
| 4.9 | Comparison of Experimental and Simulated Results..... | 48 |
| 5. | Conclusions and Future Work..... | 50 |
| 6. | References | 52 |
| APPENDIX A – Data Set | | 54 |
| APPENDIX B – Project Publications | | 65 |

LIST OF FIGURES

| | |
|--|----|
| Figure 1.1: Picture of a naturally contaminated silicone rubber insulator | 2 |
| Figure 1.2: The picture of a flashover of an insulator [5]. | 3 |
| Figure 2.1: Obenaus model of polluted insulator [10]. | 7 |
| Figure 3.1: Schematic of testing in fog chamber for surface resistance measurement | 14 |
| Figure 4.1: Time taken to reach stable conductivity values for different salts | 18 |
| Figure 4.2: Variation of surface resistance with time for the three salts | 19 |
| Figure 4.3: FOV prediction for a single standard porcelain bell (5.75"X 10") with 310 mm leakage distance artificially contaminated with different salts at an ESDD of 0.17 mg/cm ² | 19 |
| Figure 4.4: Schematic of leakage length path shown in dotted line when there is (a) no shed bridging, (b) one shed bridging and (c) two sheds bridging | 20 |
| Figure 4.5: Predicted FOV of 305" (1550 kV BIL) leakage distance post with liquid calcium chloride as contaminant with shed bridging effect (ESDD of 0.17 mg/cm ²) | 20 |
| Figure 4.6: Predicted FOV of 132" (750 kV BIL) leakage distance post with solid calcium chloride and solid sodium chloride salts as contaminants | 21 |
| Figure 4.7: Variation of FOV to ESDD for different materials | 23 |
| Figure 4.8: FOV prediction curve at 95% Prediction interval for new silicone rubber | 25 |
| Figure 4.9: FOV prediction curve at 95% Prediction interval for aged silicone rubber | 27 |
| Figure 4.10: FOV prediction curve at 95% Prediction interval for aged EPDM | 28 |
| Figure 4.11: FOV prediction curve at 95% Prediction interval for PORCELAIN | 30 |
| Figure 4.12: Comparison of experimental results of surface resistance vs. ESDD for aged silicone rubber and aged EPDM | 31 |
| Figure 4.13: Comparison of experimental results of surface resistance for a constant ESDD for aged silicone rubber with and without recovery, aged EPDM and porcelain | 31 |
| Figure 4.14: FOV prediction curve at 95% prediction interval for aged EPDM based on surface resistance | 33 |
| Figure 4.15: Insulators evaluated a) severe flashover marks b) no flashover marks | 34 |
| Figure 4.16: Measured surface resistance values of samples 1-5. | 35 |
| Figure 4.17: Sample (1) tested at 2.0 kV – no discharge (voltage drop = 167 mV) | 36 |
| Figure 4.18: Sample (4) tested at 1.5 kV– severe discharge (voltage drop = 478 mV) | 36 |
| Figure 4.19: Flow chart of proposed simulation model | 37 |
| Figure 4.20: FOV for different surface resistance vs leakage distance | 38 |
| Figure 4.21: Variation of FOV with leakage distance for different materials | 39 |
| Figure 4.22: FOV prediction curve at 95% prediction interval for aged EPDM based on leakage distance | 41 |
| Figure 4.23: FOV prediction curve at 95% prediction interval for aged silicone rubber no recovery / new EPDM based on leakage distance | 42 |
| Figure 4.24: Variation of Surface Resistance (SR) vs time for aged EPDM sample "A" with and without recovery | 43 |
| Figure 4.25: Variation of Surface Resistance (SR) vs time for aged EPDM sample "B" with and without recovery | 44 |
| Figure 4.26: Variation of Surface Resistance (SR) vs time for aged Silicone rubber sample "A" with and without recovery | 44 |

List of Figures (Continued)

| | |
|--|----|
| Figure 4.27: Variation of Surface Resistance (SR) vs time for aged silicone rubber sample “B” with and without recovery | 45 |
| Figure 4.28: Simulation model considered for porcelain..... | 46 |
| Figure 4.29: Simulation model considered for silicone rubber..... | 46 |
| Figure 4.30: Graphical representation to show simulated FOV and experimental FOV for new, aged silicone rubber and aged EPDM..... | 49 |
| Figure 6.1: Graphs showing various statistical assumptions checked for new silicone rubber model..... | 55 |
| Figure 6.2: Graphs showing various statistical assumptions checked for aged silicone rubber model..... | 56 |
| Figure 6.3: Graphs showing various statistical assumptions checked for aged EPDM model (initial analysis)..... | 57 |
| Figure 6.4: Graphs showing various statistical assumptions checked for aged EPDM model (final analysis)..... | 58 |
| Figure 6.5: Graphs showing various statistical assumptions checked for porcelain (initial analysis)..... | 59 |
| Figure 6.6: Graphs showing various statistical assumptions checked for porcelain (final analysis)..... | 60 |
| Figure 6.7: Graphs showing various statistical assumptions checked for aged EPDM..... | 62 |
| Figure 6.8: Graph showing normality assumption checked for aged EPDM | 63 |
| Figure 6.9: Graphs showing various statistical assumptions checked for aged silicone rubber no recovery / New EPDM based on leakage distance | 63 |
| Figure 6.10: Graphs showing various statistical assumptions checked for porcelain model..... | 64 |
| Figure 6.11: Graphs showing various statistical assumptions checked for silicone rubber model..... | 64 |

LIST OF TABLES

| | |
|---|----|
| Table 4.1. Comparison of simulated FOV prediction of a standard IEEE porcelain Bell based on different models (DC) | 16 |
| Table 4.2. E_p and E_{arc} used by different researchers (DC) | 16 |
| Table 4.3. Comparison of simulated FOV prediction of a standard IEEE porcelain Bell based on different models (AC) | 17 |
| Table 4.4. E_p and E_{arc} used by different researchers (AC) | 17 |
| Table 4.5. Effect of water droplets in different sheds | 21 |
| Table 4.6. Dimensional details | 22 |
| Table 4.7. Visual observations of the samples evaluated | 34 |
| Table 4.8. ESDD values in mg/cm^2 for EPDM insulators | 35 |
| Table 4.9. Matlab based simulation results | 35 |
| Table 4.10. Simulation results based on surface resistance | 37 |
| Table 4.11. Electric field simulation results for porcelain model | 47 |
| Table 4.12. Electric field simulation results for silicone rubber model | 47 |
| Table 4.13. Recommended values of various constants for different materials | 48 |
| Table 6.1. Original Data set considered developing linear regression model between Ln (ESDD) and FOV for new silicone rubber | 54 |
| Table 6.2. Original Data set considered developing linear regression model between Ln(ESDD) and FOV for aged silicone rubber | 55 |
| Table 6.3. Original Data set considered developing linear regression model between Ln(ESDD) and FOV for aged EPDM | 56 |
| Table 6.4. Original Data for developing linear regression model - Ln(ESDD) and FOV of porcelain | 58 |
| Table 6.5. Values of ESDD, FOV and Surface Resistance for aged silicone and aged EPDM. .. | 61 |
| Table 6.6. Original Data set considered developing linear regression model between Ln(Surface resistance) and FOV for aged EPDM | 61 |

NOMENCLATURE

| | |
|-----------------------|---|
| a | Arc equation exponent |
| A | Arc constant |
| AR | Area of the insulator surface in m ² |
| CMA | Calcium magnesium acetate |
| DF | Degrees of freedom |
| E _{arc} | Arc gradient |
| E _c | Critical voltage gradient |
| E _O | Breakdown strength of the dry region |
| E _p | Voltage gradient of the pollution layer |
| EPDM | Ethylene propylene diene monomer |
| ESDD | Equivalent salt deposit density |
| F | Standard “F” statistic |
| FOV | Flashover voltage |
| HV | High voltage |
| HVDC | High voltage direct current |
| I _c | Critical current |
| IEC | International electrotechnical commission |
| IEEE | Institute of electrical and electronic engineers |
| L _{arc} | Arc length |
| L _B | Total bushing length. |
| LCD | Liquid crystal display |
| LD | Leakage distance |
| LL | Lower limit of 95% prediction interval |
| MS | Mean sum of squares |
| N | Reignition constant |
| n | Exponent of the static arc characteristic |
| NCI | Non ceramic insulators |
| NSDD | Non soluble deposit density |
| P | Probability of testing the significance of null hypothesis |
| PI | Prediction interval |
| PRESS | Prediction error sum of squares |
| R ² | Residual sum of squares |
| R ² (adj) | Adjusted residual sum of squares |
| R ² (pred) | Predicted residual sum of squares |
| R _{DO} | Resistance per unit length of dry region |
| R _p | Uniform surface resistance per unit length of the pollution layer |
| R _{poln} | Series resistance of the pollution layer |
| R _{WO} | Resistance per unit length of wet region |
| S | Standard deviation |
| SE | Standard error coefficient |
| SiR | Silicone rubber |
| SR | Surface resistance |
| SS | Sum of squares |

NOMENCLATURE (CONTINUED)

| | |
|------------|--|
| T | Standard “T” Statistic |
| UL | Upper limit of 95% prediction interval |
| UV | Ultra violet |
| VO | Volume of dissolvent |
| σ_0 | Measured conductivity in S/m |

1. INTRODUCTION

1.1 OVERVIEW

High voltage insulators form an essential part of high voltage electric power transmission systems. Any failure in the satisfactory performance of high voltage insulators will result in considerable loss of capital (millions of dollars), as there are numerous industries that depend upon the availability of an uninterrupted power supply. The principle dielectrics used for outdoor insulators are ceramics and polymers. Ceramic insulators, made up of either porcelain or glass, were traditionally used in high voltage transmission and distribution lines. Since the 1960's, however, polymers have been preferred over porcelain and glass by many utilities for the housing of high voltage outdoor materials. Polymer has many benefits over ceramic such as:

- Cheaper
- Light weight
- Easy handling and installation
- Shorter manufacturing time
- Reduced breakage (non brittle characteristic)
- High impact resistance
- Greater flexibility in product design
- Resistance to vandalism

These advantages have driven the utility people to prefer polymer insulators over conventional porcelain or glass insulators. The use of polymeric materials, particularly silicone rubber and Ethylene Propylene Diene Monomer (EPDM) as weathersheds, on outdoor insulators has increased substantially in the last twenty-five years [1, 2].

The difference in material properties between ceramic and composite insulators has a significant impact on their behavior as outdoor insulators. In the case of ceramic insulators the strong electrostatic bonding between silica and oxygen results in a high melting point, resistance to chemicals and mechanical strength. Ceramic insulators are brittle and have a high value of surface free energy, which results in a greater adhesion to water. This property of ceramic insulators makes it readily wettable and consequently has a negative impact on contamination based flashover performance. *The term flashover can be defined as an unintended disruptive electric discharge over or around the insulator.* Other problems associated with porcelain insulators are puncture, vandalism and pin erosion. Contamination related power outages that are caused by dry-band arcing are major limitations with porcelain and glass [3].

Polymers are chemically weakly bonded together, and tend to decompose when subjected to heat of a few hundred degrees centigrade. The main advantage in polymers is their low values of surface energy. This forces the polymeric materials to inhibit the formation of continuous water film and causes the formation of only isolated water droplets. Polymers, like silicone rubber and EPDM, are thus hydrophobic and have the ability to limit the leakage current much better than porcelain. Hence, they have a much better contamination based flashover performance compared to porcelain [3].

1.2 CONTAMINATION FLASHOVER

Outdoor insulators are being subjected to various operating conditions and environments. Contamination on the surface of the insulators enhances the chances of flashover. Under dry conditions the contaminated surfaces do not conduct, and thus contamination is of little importance in dry periods. In cases when there is light rain, fog or dew, the contamination on the surface dissolves. This promotes a conducting layer on the surface of the insulator and the line voltage initiates the leakage current. High current density near the electrodes results in the heating and drying of the pollution layer. An arc is initiated if the voltage stress across the dry band exceeds the withstand capability. The extension of the arc across the insulator ultimately results in flashover. The contamination severity determines the frequency and intensity of arcing and thus the probability of flashover. Figure 1.1 shows the picture of a naturally contaminated silicone rubber insulator. It can be seen that the pollution level is high enough for causing a change in the natural color of the insulator.

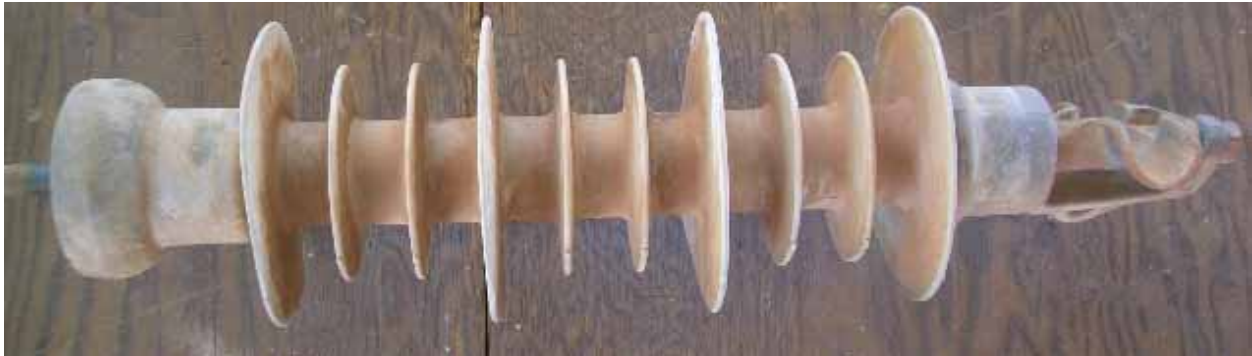


Figure 1.1: Picture of a naturally contaminated silicone rubber insulator

The economic impact that insulator flashovers exert can be severe. For example, a power outage for a quarter of a second in a paper industry would result in considerable downtime and equipment damage of up to \$50,000 [4]. Figure 1.2 shows the picture of a severe case of flashover of an insulator [5].



Figure 1.2: The picture of a flashover of an insulator [5].

1.3 NATURE OF CONTAMINANTS

In practice, there are actually various types of contaminants that tend to settle on the insulators. These contaminants can be classified as soluble and insoluble. Insulators that are located near coastal regions are typically contaminated by soluble contaminants, especially NaCl (Sodium chloride). Insulators that are located near cement or paper industries are typically contaminated by a significant amount of non-soluble contaminants. Some of the contaminants include calcium chloride, carbon and cement dust. Irrespective of the nature of the contaminant, flashover can occur as long as the salts are soluble enough to form a conducting layer on the surface of the insulator. In order to quantify the contaminants on the surface of the insulators, the soluble contaminants are expressed in terms of Equivalent Salt Deposit Density (ESDD), which correlates to mg of NaCl per unit surface area. Non-soluble contaminants are expressed in terms of Non-Soluble Deposit Density (NSDD), which correlates to mg of kaolin per unit surface area.

Apart from the above listed sources, salts that are used for de-icing streets, roads and sidewalks during winter to keep them safe for driving and walking add to the contamination problem. Salt works by lowering the freezing point of water. Ice forms when the water temperature reaches 0°C. When salt is added the temperature at which water freezes drops. A 10% salt solution freezes at -6°C, and a 20% solution freezes at -16°C. There are various road salts like sodium chloride, calcium chloride, potassium chloride, Calcium Magnesium Acetate (CMA), and magnesium chloride. Of these the most commonly used road salts are sodium chloride and calcium chloride. An assessment on the quantity of road salt used every year stated that in USA about 15 million tons and in Canada about 5 million tons of road salt is used [6, 7].

Sodium chloride, also known as rock salt, is one of the most commonly used ice melters. Compared to other materials, it has only limited effectiveness in times of very low temperatures. The main limitation is it will not melt ice at temperatures below -7°C. On the other hand, calcium chloride is actually liquid in its natural state (easy to apply) and can be converted into a dry material by removing the water. It quickly absorbs moisture from the atmosphere, while sodium chloride must come in direct contact with moisture, which is not present at low temperatures. Also, when calcium chloride is converted into liquid brine, it gives off heat. Therefore, calcium chloride will melt ice at temperatures as low as -15°C. Cost may be one of the prohibiting factors in the use of calcium chloride compared to sodium chloride [6, 7].

When applied, these road salts tend to be deposited on the surface of the insulators by the effect of wind and the movement of the vehicles. The effect that these road salts have on the insulators depends on the physical state by which they are applied to the road. Deicing streets by using liquid form of salt is the newly followed practice and is expected to have the worst effect on insulator performance.

1.4 IMPORTANCE OF SURFACE RESISTANCE MEASUREMENT (NCI)

Flashover prediction based on ESDD measurement alone may not be the best method for NCI due to its hydrophobic nature. A hydrophobic surface can have high levels of ESDD, yet the leakage current can be negligible as water formation on such a surface is in the form of discrete droplets as opposed to a continuous film. An alternate method to characterize the electrical performance was introduced based on the measurement of surface resistance under wet conditions. The use of surface resistance for predicting the flashover voltage (FOV) is explored in this work. To date there has not been much work done in characterizing the values of surface resistance that would be indicative of either flashover or withstand. It is also understood that the type of fog and rate of wetting of the insulators affects the surface resistance of NCI. It is much easier to measure ESDD than surface resistance. Thus there is a need to determine the correlation between ESDD and surface resistance. Studies have also found that the silicone rubber insulators have a higher surface resistance over the EPDM insulators. The guidelines for surface resistance measurements in laboratories under various possible test conditions are well defined [8, 9].

1.5 NEED FOR WORK IN FLASHOVER PREDICTION (ESPECIALLY FOR NCI)

In the USA, presently, non-ceramic materials are used extensively for termination of distribution cables. Currently, non-ceramic insulators have captured the power market to about 35% of the transmission line system. The increasing demand for the use of polymeric insulators and their relatively less on field experience compared to porcelain triggered the need for more research in this area. It should be noted that at present there are no standardized tests for understanding the contamination flashover performance of polymeric insulators. Based on these facts it is of utmost importance to devise an improved method to predict the FOV of an insulator based on the level of contamination.

For new construction, relevant field experience may not be available and laboratory experiments are often time consuming and expensive. A good theoretical model for simulating the flashover process is a big asset as it helps minimize experimental efforts. This research is therefore aimed at developing models by which the FOV based on contamination are to be predicted and the dynamics of flashover to be explained in cases of both highly and non-uniformly contaminated insulator.

2. FLASHOVER THEORY, EVALUATION AND MEASUREMENT OF CONTAMINATION

2.1 FLASHOVER MECHANISMS - GENERAL THEORY AND OBENAU'S MODEL

During wet atmospheric conditions like light rain or fog the contamination layer on the surface of the insulator gets wet and promotes leakage current flow along the surface. The heat dissipated due to the flow of leakage current evaporates the moisture on the surface of the insulator. This evaporation leads to the formation of areas termed as “dry bands.” Dry bands tend to form near the surface of the insulator parts where the diameter is the smallest, because of the high current density in those parts. A concentration of voltage stress is formed around the dry bands as the surface resistance of the dry bands is much higher than the conductive contaminated surface film. Subsequently the dry band will break down causing an initial partial arc over the surface. After the formation of a partial arc the propagation of the arc further depends on if $E_p > E_{arc}$, that is the arc will propagate if the voltage gradient ahead of the arc, which is the voltage gradient of the pollution layer, is greater than that of arc gradient. This is due to the fact that ionization of the path ahead of the arc by the increasing current at every instant enables the arc to proceed. When the arc propagation across the contaminated layer bridges the whole insulator a flashover will occur. The flashover triggers a power arc that results in the interruption of power supply and may damage the insulator temporarily or permanently, depending on the severity of flashover [10 - 16].

Though the study of the process of contamination flashover has been done for many decades at different labs and at outdoor locations across the world, the understanding of the physical process is not complete even now. This can be attributed to the intense complexity involved in the flashover process. Also, the numerous parameters involved in the process of flashover make it even more difficult to understand the process completely. As an example it has been observed in service that FOV depends upon various factors but is not limited to such as, the polarity of voltage, particle size, non-uniform wetting, the size and nature of the pollutant surface conductivity, wind, washing, length, orientation, diameter and profile of the insulator.

Obenaus was the first to propose a model for contamination flashover. Obenaus outlined the steps that were required to calculate the FOV [12]. The actual computation was completed by Neumarker who derived an expression that relates FOV and surface conductivity [13]. In this theory flashover process is modeled as a discharge in series with a resistance as shown in Figure 2.1. Here the discharge represents the arc bridging the dry band, and the resistance represents the un-bridged portion of the insulator. The voltage drop across the resistance is taken as a linear function of current. The equations derived for critical voltage gradient (E_c) and critical current (I_c) are [17-20],

$$E_c = N^{(1/(a+1))} * R_p^{(a/(a+1))} \quad (1)$$

$$I_c = (N/R_p)^{(1/a+1)} \quad (2)$$

where

$R_p = R_{poln} / (LD - L_{arc})$, uniform surface resistance per unit length of the pollution layer

N = Reignition constant

a = Arc equation exponent

R_{poln} = Series resistance of the pollution layer

LD, L_{arc} = Leakage distance and arc length respectively.

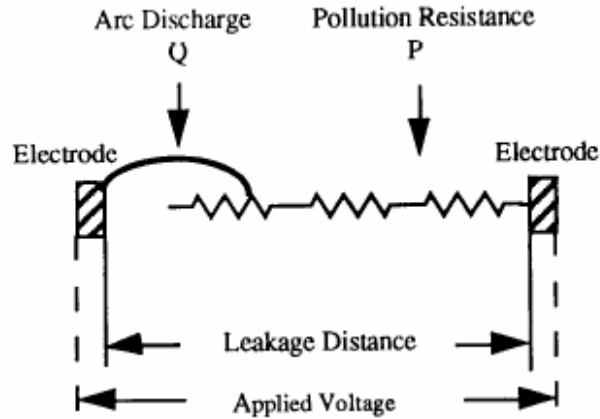


Figure 2.1: Obenaus model of polluted insulator [10]

2.2 FLASHOVER THEORY OF VARIOUS OTHER RESEARCHERS

Various other researchers have proposed alternative models to that of Obenaus. Hampton proposed a theory on the basis of an experiment in which he used a water jet to simulate a contaminated long rod insulator [14]. According to Hampton's theory, FOV was treated primarily as a stability problem. Hampton stated that an unstable situation occurs if there is a current increase when the discharge root is displaced in the direction of flashover. From this he concluded that if the voltage gradient along the discharge was ever to fall below the gradient along the resistive column, then flashover would occur. Subsequently it was mathematically proven by Hesketh that Hampton's two criteria of voltage gradient and current increase were identical only in the case of a long rod insulator [15].

Alston and Zoledaiowski later on proposed an algebraic derivation for the critical conditions of flashover [16]. They incorporated the discharge length in the condition of flashover. According to their theory the voltage required to maintain local discharges on polluted insulators may increase with an increase in discharge length. If this voltage exceeds the supply voltage then the discharge extinguishes without causing a flashover. An equation was proposed that defines the critical relation between the applied stress and the resistance of the pollution for DC voltages. According to the equation, flashover cannot occur if:

$$E_c < 10.5 * R_{poln}^{0.43} \quad (3)$$

Numerous authors who worked in this field proposed various equations by varying the empirical constant, and calculations of FOV based on each model yielded a different value. Rizk proposed a similar equation for AC voltages which is given by [17],

$$E_c < 23 * R_{poln}^{0.40} \quad (4)$$

In Equation (4) the increase in the constant of proportionality is attributed to the arc extinction due to natural current zeroes, which inhibits arc elongation.

Most of the models studied so far are static in nature in the sense there is no arc propagation criterion accounted for in these models. The static models assume that once the arc is initiated it propagates unextinguished. Thinking in terms of reality, arc propagation is a rapid time varying phenomena, an arc will propagate only when conditions are conducive. Static models do not consider variations in arc and pollution resistance and arc current with time. These limitations in static models led to the development of dynamic models.

The dynamic model was initially proposed by Jolly, Cheng and Otten [19]. In this model the arc propagation criterion used was the variation in arc electrode gap. With this model it was possible to predict the time to flashover for electrolyte strips. Even though a good correlation was observed on one dimension, it was defective for 2D and 3D. Subsequently, various authors, including Rizk, proposed dynamic models. However significant improvement in the development of a dynamic model was undertaken by Raji Sundararajan. In her work the various factors like arc propagation criteria, change in arc parameters with time, effect of various contaminants on flashover and the role of geometry, were all considered [20].

2.3 FLASHOVER THEORY IN PARTIALLY CONTAMINATED INSULATORS

Apart from the various theories discussed so far regarding a uniformly contaminated insulator, flashover, was observed also in a partially or a non-uniformly contaminated insulator. In many insulators flashovers have taken place without any indication of surface discharge activity. The FOV is much lower than predicted by clean fog. High non-uniform voltage distribution is believed to trigger streamer discharges. Some significant observations in this type of flashover termed as sudden flashover are [21- 24]:

- In streamer discharge FOV is non-linear to leakage distance.
- The high resistance region near the HV end causes higher field intensification
- Insulators with smaller shed spacing suffered a significant reduction in performance as smaller shed spacing may itself aid an arc to jump
- In contrast to wholly contaminated insulators the path of the arc is essentially through air instead of following the leakage distance path
- Hanging water droplets due to rain may substantially reduce dielectric strength between sheds
- Complete shed bridging due to water bridging the gap
- Ratio of the resistance/unit length of wet region to dry region is a key parameter for prediction

Some possible solutions that are sought of for this problem include but are not limited to:

- Insulator shapes are to be modified with the aim of an improved contamination performance
- Improvement of insulator materials improves the performance (NCI better than ceramic)
- Increase in shed spacing as typically observed in NCI

2.4 MEASUREMENT OF CONTAMINATION SEVERITY

Contamination severity on the surface of insulators can be given in terms of ESDD as explained earlier. The measurement of ESDD in case of porcelain and glass has been standardized in the International Electrotechnical Commission (IEC) document 60507

ESDD is measured by dissolving the contaminants on the surface of the insulators, in deionized water and then measuring the conductivity of the water. The ESDD is then calculated using the following formula

$$\sigma_{20} = \sigma_{\theta} (1 - b (\theta - 20)) \quad (5)$$

σ_{θ} - The measured conductivity in S/m.

b - 0.01998 (constant)

$$ESDD = (5.7 * \sigma_{20})^{1.03} * VO / AR \quad (6)$$

VO- Volume of dissolvent (distilled water) in m³

AR- Area of the insulator surface in m²

This method is observed to be good for measuring ESDD for porcelain and glass insulators, as these are completely wettable [9].

2.5 EVALUATION OF CONTAMINATION FLASHOVER PERFORMANCE IN LABORATORIES

The properties of polymer insulators tend to change with time because of longtime exposure to UV (Ultra Violet) rays from sunlight, temperature, mechanical loads and electrical discharges in the form of arcing or corona. Such a reduction in the electrical and mechanical properties is termed aging. The silicone rubber insulators tend to lose one of their most important properties of hydrophobicity when they are continually subjected to various extreme levels of environmental factors. The various characteristics of the insulators can be evaluated by the records obtained from service. Though the records from the field are of immense value, they are difficult to obtain and may take a long period of time before their validity can be proved. As a result laboratory tests are increasingly used to evaluate the various performance characteristics of the insulators to correlate with actual field conditions.

Laboratory results are used by most of the manufacturers to determine the design and material selection of insulators. They are used by transmission engineers to determine the design of transmission lines and the insulators to be used on those lines. The most common tests that are employed for the evaluation of non-ceramic insulators are the clean fog and salt fog test. These tests are standardized for ceramic insulators and are referred to as fog chamber tests.

The clean fog chamber tests involve the pre-contamination of the insulator with slurry made of conductive salt usually sodium chloride and an inert clay binder (kaolin). Then the insulator is subjected to wetting by steam. This simulates the field condition in which the insulator is first contaminated and then wetted. In the case of a salt fog test a clean insulator is energized in the fog chamber using fog produced from saline (NaCl) water. This test simulates the field condition in which the clean insulator is subjected to contamination in a salty environment as it happens in coastal areas. The service condition can be varied by the applied voltage, the rate of wetting and the amount of contamination, depending on the requirement. All these parameters are observed to have significant effect on the performance of the insulator.

2.6 SURFACE RESISTANCE FOR CHARACTERIZING FLASHOVER

The measurement of surface resistance in the case of non-ceramic insulators during wet conditions is a useful technique to characterize the contamination performance and aging. Silicone insulators, due to their hydrophobic nature, may perform satisfactorily during wet conditions. In those cases the surface resistance, calculated from the leakage current measured, acts as a true representative of the contamination performance of the insulator. In reality surface resistance has been used as a key parameter to model flashover. One example of such a model assumes a dry zone of varying length, which is used to determine the conditions that may lead to flashover in HVDC (High Voltage Direct Current) wall bushings in non-uniform rain. In this model the ratio of the resistance per unit length of wet region to dry region is used as a key parameter. Surface resistance measurements can be utilized to evaluate the potential capability of various materials to prevent HVDC wall bushing flashover in conditions of non-uniform rain. The above model which analyzed the voltage distribution across wet and dry zones, accounts for the breakdown strength of the dry zones leading to the following necessary condition for flashover in HVDC wall bushing [22]:

$(R_{WO} / R_{DO}) < (V_S / E_O L_B)$; where

R_{WO} and R_{DO} are the resistance per unit length of wet and dry regions respectively

E_O is the breakdown strength of the dry region, L_B is the total bushing length.

Surface resistance generally reflects multivariables, which are typically the type of material, wetting rate, ESDD and the recovery characteristic. The surface resistance of the insulator that has recovered is different from the surface resistance of the un-recovered insulator particularly for the silicone rubber type. Apart from these, surface resistance can be used to assess the aging of the insulating materials. Aging of insulating materials can be defined according to IEC and IEEE standards, as the ‘*occurrence of irreversible deleterious changes that critically affect performance and shorten useful life.*’ Aging is a complicated process. Aging would lead to increased leakage current and subsequent flashover of insulators during wet and

contaminated conditions. Quantifying and comparing aging in non – ceramic insulators is not a simple task. As aging leads to increased leakage current, it can be assumed that surface resistance measurements can be used as indicators to quantify and compare aging in case of NCI.

A task force of the IEEE working group on insulator contamination by R. S. Gorur, et al [9] determined whether surface resistance measurements can be formalized to ensure repeatable and reproducible results for both silicone and EPDM. A porcelain post insulator was used as a reference for the analysis. For the above study surface resistance was measured both in artificially contaminated and in “as received” conditions. Fog wetting and spray wetting were the methods of wetting used. The study finally concluded that it is possible to establish a standard for surface resistance measurements in the laboratories. The study also issued useful guidelines for surface resistance measurements like insulator orientation, voltage to be applied, duration of test and method of wetting.

3. EXPERIMENTAL SET UP

3.1 FOG CHAMBER DESCRIPTION

The experiments in this research work involved the estimation of ESDD, measurement of surface resistance and estimation of flashover of porcelain and polymer insulators namely silicone rubber and EPDM. The fog chambers are in general used for various artificial contamination tests of porcelain, glass and non-ceramic insulators under different simulated environmental conditions. Various experiments were carried out in the fog chamber available at the high voltage laboratory in ASU.

The fog chamber used for these experiments is made of stainless steel sheets and its dimensions are 3.66 X 3.05 X 2.44 m which makes it a volume of approximately 27 m³. There are four IEC dimensioned fog nozzles present, one on each wall of the chamber inside. The HV supply is provided by a transformer rated at 40 kVA/100 kV located outside the fog chamber. A water boiler is located inside the fog chamber for the generation of steam fog. The water source for the air nozzle is a water drum outside the chamber. The condensed water inside the chamber is circulated out to the drain using a pump that is operated by a timer by which water can be pumped out every 15 minutes. For the visual observation of the fog chamber a 30 X 20 cm glass window is fitted on the door.

Three different modes of fog generation that are available for the experiments are:

- 1) Salt fog generated by the standard IEC 507 nozzles
- 2) Steam fog generated by the boiler that is inside the chamber
- 3) Fog generated by ultrasonic fog generators.

The water is boiled in a vat to produce a steam input rate of about 50 - 250 g/m³/h. In this work ultrasonic nebulizers were used to generate fog. The size of the droplet generated by the nebulizer is very small typically 1 micron in diameter. These devices are easy to maintain, consume less power and minimize corrosion problems encountered with conventional fog generators like boiling water or salt spray. A relative humidity level of 100% was achieved within 20 minutes of energizing the fog generators.

3.2 ARTIFICIAL CONTAMINATION OF NON CERAMIC INSULATORS

An examination of insulators that were in the field for a long time and exposed to various contaminants indicates that the contamination is dispersed fairly uniformly. Based on this it is important to make sure that a uniform layer of contamination is applied on the insulators for the experiments. The contamination slurry to be applied on the insulator is obtained by mixing 40g of kaolin in one liter of deionized water. Kaolin acts as the binder in the slurry. No other wetting agent is used in the slurry, as it may affect the surface characteristics of the non-ceramic insulator. An appropriate amount of *NaCl* was added to the slurry depending on the level of ESDD to be obtained. Using brush a uniform coating of contamination was applied on the insulator. If the required level of ESDD is not obtained from the process, then the process is

repeated again with further addition of sodium chloride to the slurry and reapplication on the insulator to get the required ESDD. There was several hours elapsed from the time the surface was dry to the time at which they were tested. This allowed recovery of hydrophobicity of silicone rubber to various degrees depending on the time elapsed. Samples were tested when the surface had no recovery of hydrophobicity (1 hour after drying), and visibly recovered its hydrophobicity (3 days after drying). Recovery was judged by spraying water and noting if the surface wetted out or beaded in to small drops and conclusions were made based on STRI guide 92/1. The EPDM samples were always hydrophilic and there was no visible recovery of the hydrophobicity with time.

3.3 MEASUREMENT OF SURFACE CONDUCTIVITY AND CALCULATION OF ESDD

After the artificially contaminated insulators are dried, the surface conductivity is to be measured to calculate the ESDD. A compact portable contamination measurement unit is used to measure the conductivity on the surface of the insulator. It basically consists of a measurement cell mounted on a vise grip that can be fixed on most of the insulator surfaces. The measurement cell is made of a plexiglass tube that is sealed with an O-ring at the lower perimeter to make it water tight when it is fixed on the surface of insulator. The surface area of the measurement cell is approximately 1.8 cm².

The conductivity of the insulator surface where the instrument is placed is measured as follows:

- 1) The portable device is fixed on the surface of the insulator and is filled with 1.8 ml of deionized water.
- 2) The deionized water is allowed to remain on the surface of the insulator for about two minutes. After two minutes the water is siphoned off using a syringe and this is again siphoned onto the surface so that the contaminant dissolves properly. This process is repeated for about five times to get an accurate assessment of conductivity.
- 3) The conductivity of the removed water is then measured using a calibrated digital conductivity meter (B-173).
- 4) This whole process is repeated on different insulator sheds to ensure that insulators have been contaminated uniformly.
- 5) ESDD is then calculated from the measured conductivity using the formula explained earlier in section 2.4

The conductivity meter used (B-173) has a digital LCD that indicates the conductivity directly. The conductivity meter can be used to measure a wide range of conductivity varying from 0 – 19.9 mS/cm. The conductivity meter is rinsed in the washing liquid (purified water) and calibrated periodically using a standard solution of 1.41 mS/cm. in order get accurate measurements.

3.4 TESTING PROCEDURE FOR SURFACE RESISTANCE MEASUREMENT AND ESTIMATION OF FOV

AC voltage in the range of 2-4 kV was used depending on the insulator material and dimensions. The voltage was applied across aluminum tape electrodes that were placed in between the insulator hardware. The leakage distance of the insulators between the electrodes was typically 15 cm. The voltage applied should be adequate to establish a measurable leakage current but not high enough to initiate discharges. The insulators were mounted vertically in the chamber. Figure 3.1 shows the schematic of testing. Care is taken to ensure that the source of fog generation is not directly beneath the sample. The data acquisition system for the leakage current consists of an oscilloscope in which there are three options of resistance 100 Ω , 470 Ω and 1 k Ω . The leakage current is measured as a voltage drop across the resistor connected in series with the sample. The surface resistance is calculated based on the fact that the applied voltage is the sum of the voltage drop across the sample and resistor. The surface resistance value is high initially and a steady value of surface resistance was obtained in 70-90 minutes after starting the fog generators

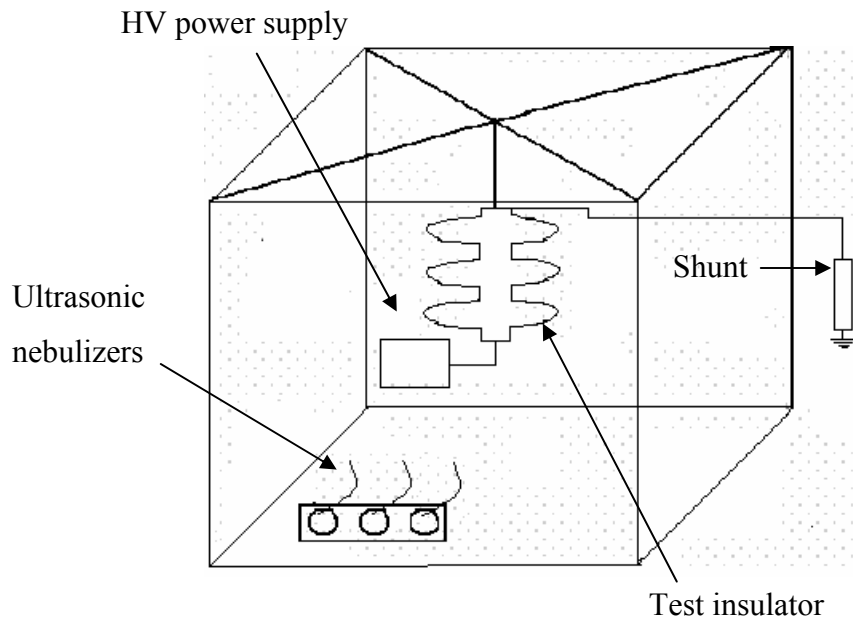


Figure 3.1: Schematic of testing in fog chamber for surface resistance measurement

Most of the experiments performed in this work measured the surface resistance of different samples at different values of ESDD. Moreover, FOV for different levels of ESDD were estimated. To measure FOV, the insulator is subjected to 80% of the probable FOV (determined from previous trials) for 20 minutes after the relative humidity has reached 100%. If there is no flashover the voltage is raised in 10%, and each step is maintained for 5 minutes until flashover is obtained. This process is repeated for different levels of ESDD. The FOV reported is the average of three measurements for the same ESDD. A different sample of the same type was used for different trials.

4. RESULTS AND ANALYSIS

4.1 COMPARISON OF SIMULATED RESULTS OF VARIOUS ARC MODELS

As discussed in Section 2.2 there are numerous models that have been proposed for predicting the FOV. Various researchers have proposed numerous models based on different empirical values for constant and exponent of static arc characteristic. In order to investigate how close the predictions are by different authors, various models were simulated by keeping Sundararajan model (Researcher A) as the basis of comparison [18, 20, 25]. The simulation results for DC and AC models are presented in Table 4.1 and Table 4.3 respectively. The E_{arc} and E_p equations used by different researchers for DC is given in Table 4.2 and for AC in Table 4.4. The dimensional details of the standard IEEE porcelain bell considered for simulation are leakage length of 28 cm, shed diameter of 25.4 cm and unit spacing of 14.6 cm. The equations that were used as basis for simulation for DC models (equations 7 and 8), AC models (equations 7 and 9) are given as

$$E_{arc} = N \times I^{-n} \quad (7)$$

$$E_p = E_c = A^{1/a+1} \times rpu^{a/a+1} \quad (8)$$

$$E_p = E_c = 10 * N \times (N - A)^{-n/n+1} \times n^{n/n+1} \times rpu^{n/n+1} / n+1 \quad (9)$$

Where

n - Reignition exponent (typically 0.5)

A - Arc constant (typically $0.15 * N$)

I - Current entering the pollution layer

rpu - average resistance per unit length

The Matlab programs that were developed based on the flowchart developed by Sundararajan for these simulations are given in Appendix titled “Matlab programs” [10, 20]. The values of the various constants and the arcing model equations that were used for simulations are from references [10, 18, 20, 25] and are provided in the Appendix. It can be inferred from Table 4.1 that the variation of prediction for FOV is a very wide range from 0% to as high as 170%. In case of AC models with Rizk’s model (Researcher E) as reference for comparison the variation of prediction for FOV is from 2% to about 90%. Hence, it can be observed that there is a very wide range of prediction and it is very difficult to predict the exact FOV.

Table 4.1. Comparison of simulated FOV prediction of a standard IEEE porcelain Bell based on different models (DC)

| ESDD (mg/cm ²) | Researcher A | Researcher B | Researcher C | Researcher D |
|-------------------------------|--------------|--------------|--------------|--------------|
| Light | (kV) | (kV) | (kV) | (kV) |
| 0.01 | 14.6 | 12.0 | 14.2 | 28.0 |
| 0.02 | 11.8 | 11.0 | 11.8 | 24.6 |
| 0.03 | 10.4 | 10.4 | 10.6 | 22.8 |
| 0.04 | 9.6 | 10.0 | 9.8 | 21.6 |
| Moderate | | | | |
| 0.05 | 9 | 9.8 | 9.2 | 20.8 |
| 0.06 | 8.5 | 9.6 | 8.8 | 20.2 |
| 0.07 | 8.1 | 9.1 | 8.4 | 19.6 |
| 0.08 | 7.8 | 9.2 | 8.2 | 19.0 |
| Heavy | | | | |
| 0.10 | 7.3 | 9.0 | 7.8 | 18.4 |
| 0.12 | 6.9 | 8.8 | 7.4 | 17.8 |
| 0.15 | 6.5 | 8.6 | 7.0 | 17.0 |
| 0.20 | 6.0 | 8.2 | 6.4 | 16.2 |

Table 4.2. E_p and E_{arc} used by different researchers (DC)

| | Researcher A | Researcher B | Researcher C | Researcher D |
|------------------|--------------------|---------------------|----------------------|-----------------------|
| E_p (V/cm) | $15.83 * Rp^{0.4}$ | $28.5 * rpu^{0.43}$ | $20.1 * rpu^{0.296}$ | $24.58 * rpu^{0.194}$ |
| E_{arc} (V/cm) | $63 * I^{(-0.5)}$ | $37.2 * I^{(-0.5)}$ | $15.93 * I^{-0.42}$ | $312.7 * I^{-0.24}$ |

Table 4.3. Comparison of simulated FOV prediction of a standard IEEE porcelain Bell based on different models (AC)

| ESDD (mg/cm ²) | Researcher E | Researcher F | Researcher G | Researcher H |
|-------------------------------|--------------|--------------|--------------|--------------|
| Light | (kV) | (kV) | (kV) | (kV) |
| 0.01 | 12.0 | 20.2 | 12.2 | 22.6 |
| 0.02 | 10.6 | 16.2 | 10 | 18.2 |
| 0.03 | 9.8 | 14.2 | 8.8 | 16 |
| 0.04 | 9.2 | 13.0 | 8.0 | 14.6 |
| Moderate | | | | |
| 0.05 | 9.0 | 12.2 | 7.6 | 13.6 |
| 0.06 | 8.6 | 11.6 | 7.2 | 13.0 |
| 0.07 | 8.4 | 11.0 | 6.8 | 12.4 |
| 0.08 | 8.2 | 10.6 | 6.6 | 11.8 |
| Heavy | | | | |
| 0.10 | 8.0 | 9.8 | 6.2 | 11.0 |
| 0.12 | 7.6 | 9.4 | 6 | 10.4 |
| 0.15 | 7.4 | 8.8 | 5.6 | 9.8 |
| 0.20 | 7.0 | 8.0 | 5.2 | 9.0 |

Table 4.4. E_p and E_{arc} used by different researchers (AC)

| | Researcher E | Researcher F | Researcher G | Researcher H |
|------------------|-----------------|---------------------|---------------------|----------------------|
| E_p (V/cm) | $58*rp_u^{0.4}$ | $103.3*rp_u^{0.33}$ | $63.4*rp_u^{0.333}$ | $113.6*rp_u^{0.333}$ |
| E_{arc} (V/cm) | $59*I^{(-0.5)}$ | $80*I^{(-0.5)}$ | $37.78*I^{-0.5}$ | $94*I^{-0.5}$ |

4.2 ANALYSIS OF TEST RESULTS OF DIFFERENT ROAD SALTS

As mentioned earlier, road salts, which are applied for deicing purposes, get deposited on the insulator and considerably deteriorate the performance. In order to study their effect, three types of salts namely solid calcium chloride, solid sodium chloride and liquid calcium chloride were considered. As a first assessment, the time taken by each salt to reach a stable comparable conductivity was noted. A graphical variation of time taken to reach stable conductivity values for different salts is shown in Figure 4.1. From observing Figure 4.1 it can be expected that once the road salts get deposited onto the surface of insulators the liquid salt will have considerable effect in early stages compared to other salts. To confirm this, they were applied on a standard porcelain bell of dimension (5.7" X 10") of leakage length 12.2". All the three samples were tested at an ESDD of 0.17 mg/cm² and the surface resistance was measured as shown in Figure 4.2. The applied voltage was 2 kV in all the cases. In Figure 4.2 the Y axis represents surface resistance measured in MΩ per cm of leakage distance. It can be observed that application of

liquid salts on the road has an immediate, more deleterious effect than other salts. The liquid salt has enough moisture resulting in an immediate lower surface resistance whereas for solid salts it requires some time to acquire. Figure 4.3 shows the FOV calculation for a single standard porcelain bell (5.75" X 10") with a leakage distance of 310 mm. It can be observed that at the starting point there is a 56% decrease in FOV with liquid salt compared to solid CaCl_2 , and 28% decrease in FOV compared to solid NaCl . This fact quantitatively substantiates the deleterious effect of liquid salt on flashover performance

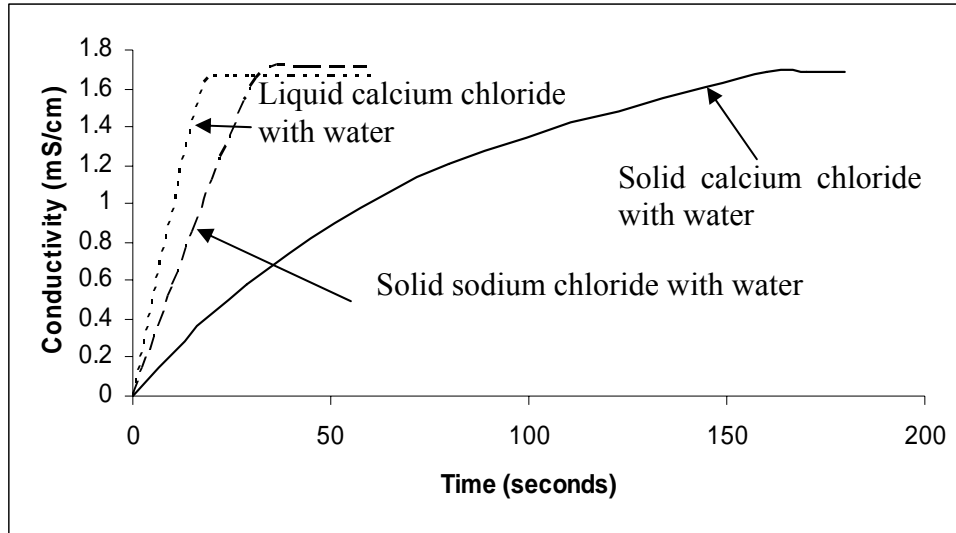


Figure 4.1: Time taken to reach stable conductivity values for different salts

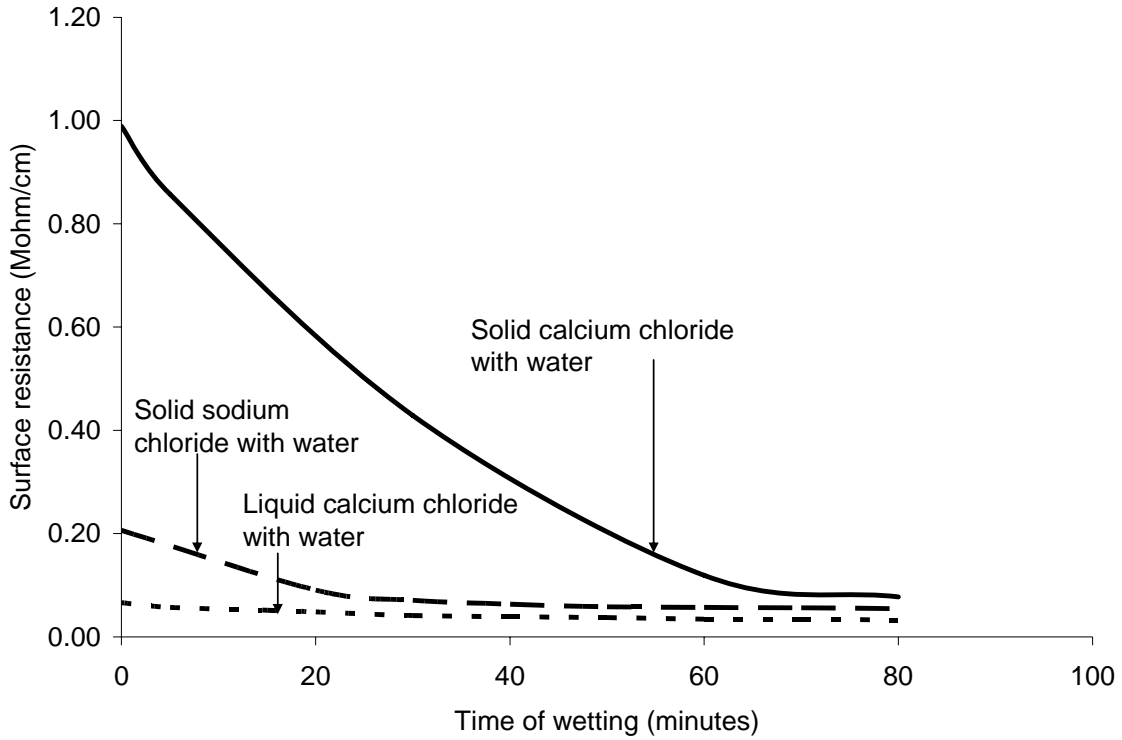


Figure 4.2: Variation of surface resistance with time for the three salts

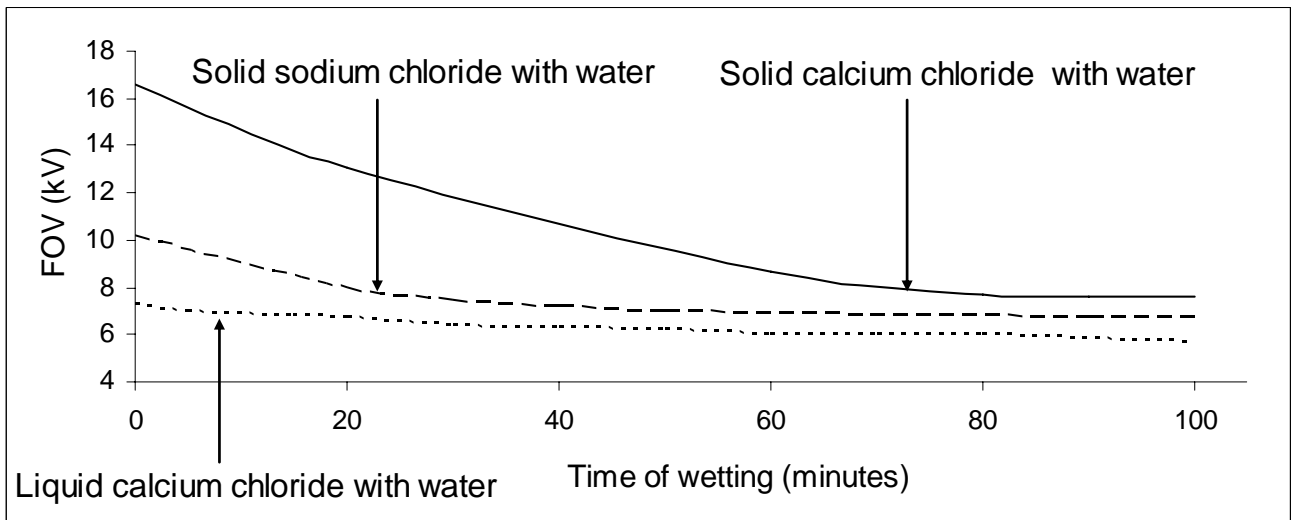


Figure 4.3: FOV prediction for a single standard porcelain bell (5.75"X 10") with 310 mm leakage distance artificially contaminated with different salts at an ESDD of 0.17 mg/cm²

In order to understand the effect of shed bridging on further lowering the FOV different scenarios as shown in Figure 4.4 were considered for FOV prediction

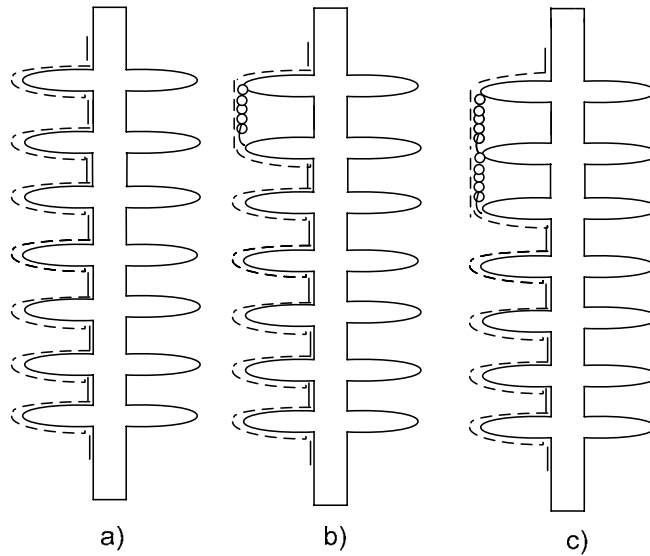


Figure 4.4: Schematic of leakage length path shown in dotted line when there is no shed bridging (a), one shed bridging (b) and two sheds bridging (c)

Figure 4.5 shows the predicted FOV of 305" leakage distance post for liquid calcium chloride considering shed bridging effect. It can be observed that while the insulator is not expected to flashover in normal operating conditions whereas with three shed bridging it will flashover. Figure 4.6 shows the predicted FOV of 132" leakage distance post with solid calcium chloride and solid sodium chloride salts as contaminants. With the nominal operating voltage of 230 kV the insulator is expected to withstand and not flashover if solid calcium chloride is the contaminant but will flashover if solid sodium chloride is the contaminant. Thus it is evident that the performance of insulators with solid calcium chloride is much superior to solid sodium chloride salt. The simulations to obtain graphs of Figs 4.5 and 4.6 were done in Matlab.

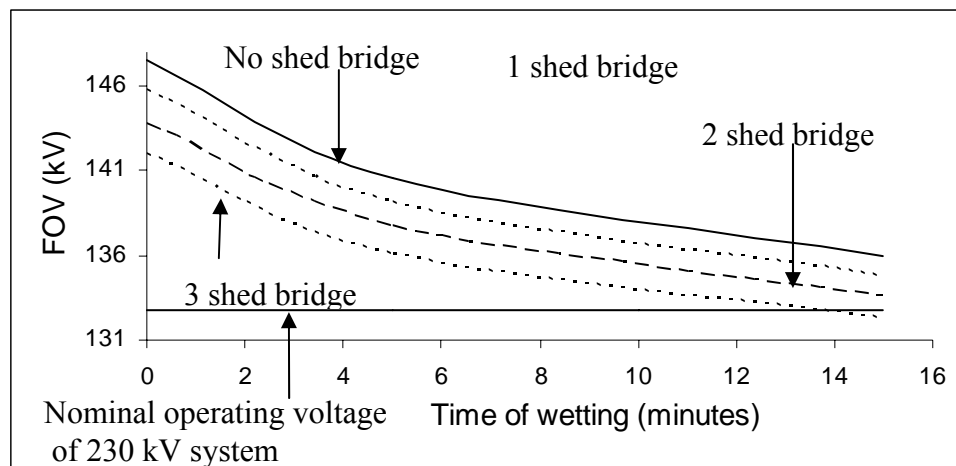


Figure 4.5: Predicted FOV of 305" (1550 kV BIL) leakage distance post with liquid calcium chloride as contaminant with shed bridging effect (ESDD of 0.17 mg/cm²)

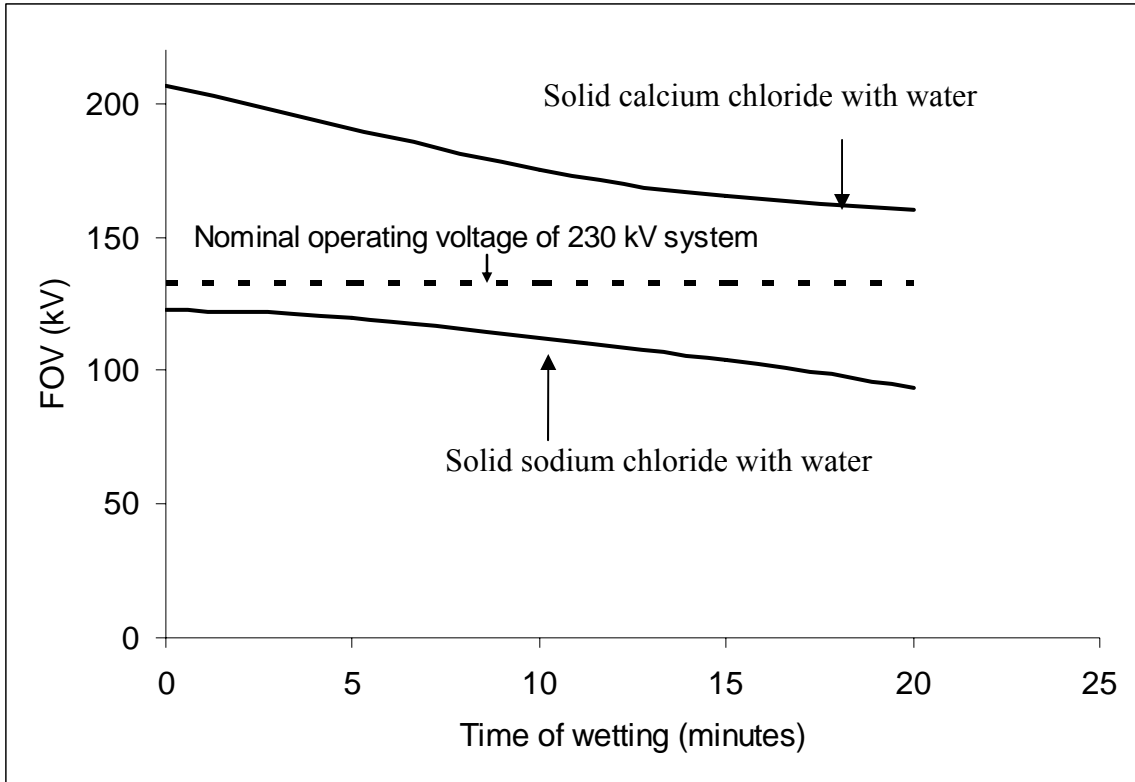


Figure 4.6: Predicted FOV of 132” (750 kV BIL) leakage distance post with solid calcium chloride and solid sodium chloride salts as contaminants

4.3 EFFECT OF WATER DROPLETS IN DIFFERENT SHEDS

In order to further understand, the intensification of E-field at the tip of junction of water droplet and shed was modeled using coulomb. Two cases were considered. First is the change in E-field with the increase in number of water droplets in a same shed. Secondly, considering the same scenario in subsequent sheds (away from HV end). The results obtained for the geometry of a 5 shed insulator with leakage distance 133.5 cm, shed diameter 12 cm, and a shed spacing of 10 cm is given in Table 4.5. The radius of water droplet considered was 0.25 cm.

Table 4.5. Effect of water droplets in different sheds

| Shed Position | Number of water droplets | E field increase in% compared to no water droplet |
|---------------------|--------------------------|---|
| First shed | One droplet | 33.33 |
| (closest to HV end) | Four droplets | 85.55 |
| Second shed | One droplet | 6.1 |

Following are the observations from Table 4.5.

- In any shed the increase in number of water droplets shows an increase in E- field at the tip of the shed
- As we move away from the HV end towards ground end the increase in E-field value at the water droplet/shed junction is significantly lower than observed for the shed which is closest to HV end.

4.4 DEVELOPMENT OF A MODEL TO PREDICT FOV BASED ON ESDD VARIATION FOR NON-CERAMIC AND CERAMIC INSULATORS

In order to understand the effect of variation of ESDD to FOV, a series of experiments were performed on new and field-aged samples of insulators using silicone rubber and ethylene propylene diene monomer (EPDM) rubber as housing materials. The insulator shapes were identical. Porcelain line post insulators with a geometry as close to that of the NCI was used as a reference. The field-aged samples were removed after 5 years of exposure in the mid west USA. It is important that the period of field exposure and the service location be similar for comparison of different material types. The aged silicone samples were still hydrophobic but the EPDM samples had lost its initial hydrophobicity. The hydrophobicity was assessed visually by using STRI guide 92/1. There was surface discoloration of the aged EPDM samples most likely from ultraviolet radiation in sunlight. There was no visible degradation on the aged samples. The experiments were performed with ESDD values as low as 0.08 mg/cm² to 0.34 mg/cm². The dimensional details of the samples tested are provided in Table 4.6. Figure 4.7 shows the experimental results for the variation of ESDD vs FOV for all the four material types. It can be seen that for the same level of ESDD the FOV for an aged silicone rubber is about 12% less compared to new silicone rubber. The aged EPDM has a FOV of about 16% lower than aged silicone rubber, whereas porcelain has a FOV of about 16% lower than aged EPDM. These differences in the FOV are indicative of inherent differences in the materials' ability to resist water filming.

Table 4.6. Dimensional details

| Type of material | Leakage distance (cm) | Shed diameter (cm) | Shed spacing (cm) |
|----------------------|-----------------------|--------------------|-------------------|
| New silicone rubber | 27.0 | 9.0 | 3.0 |
| Aged silicone rubber | 27.0 | 9.0 | 3.0 |
| Aged EPDM | 26.0 | 9.0 | 2.0 |
| Porcelain | 25.0 | 13 | 2.0 |

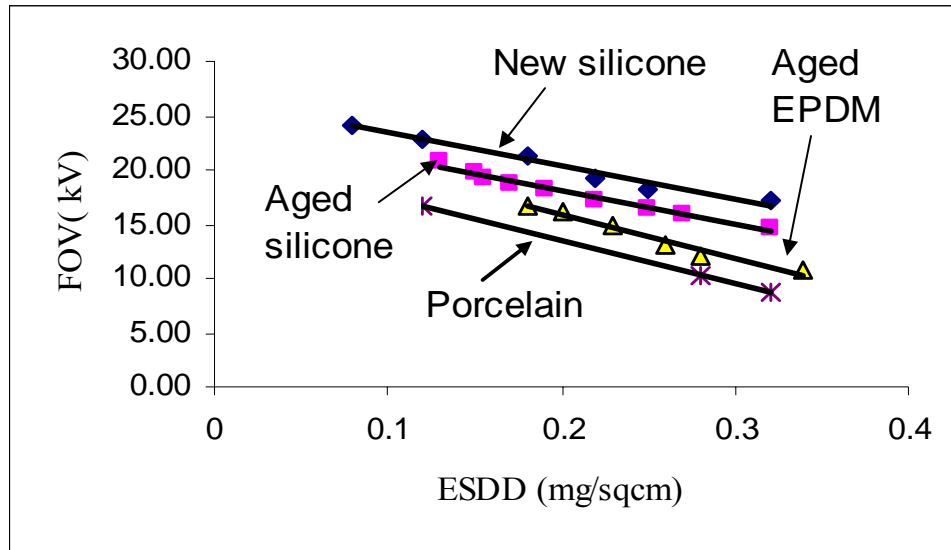


Figure 4.7: Variation of FOV to ESDD for different materials

Although most of the tests have been made at very high levels of ESDD it is possible to fit a regression model and predict with a high prediction interval of 95% the FOV for low levels of ESDD where experiments cannot be performed. Even though, in general it might be a risk to extrapolate, if the fitted regression model can be validated at some point where it has been extrapolated it can be considered to be a valid model. A regression model was initially developed for new silicone rubber material considering data points for ESDD ranging from 0.12 – 0.32. The developed regression model is valid only when certain assumptions are true. The basic assumptions to be checked are:

- Errors are normally distributed – Checked through normal probability plot of residuals
- Errors have zero mean and constant variance – Checked through plot between residuals and predicted values
- Errors are uncorrelated – Checked through plot between residuals and run order.

With regard to normal probability plot of residuals, the residuals should lie approximately in a straight line. If that is so, then it can be inferred that there is no considerable deviation from normality. Typically, a random scatter of points is obtained when the assumption of constant variance is satisfied. That is, the plot between the residuals and predicted values should not indicate any specific shape. In the plot, between residuals and run order there should not be any trend discernable from the plot. If so, the assumption of independence of errors is not violated. All the assumptions were checked and found satisfied and hence the developed model is a valid model [26 27]. Details of the data set for this model and for various models that follow this and the graphs to support assumptions for all the models are listed under Appendix – Data set.

a) New silicone rubber housing

Regression Analysis: FOV versus Ln (ESDD) for new silicone rubber

The regression equation is
FOV = 10.2 - 6.02 Ln (ESDD)

| Predictor | Coef | SE Coef | T | P |
|-----------|---------|---------|--------|-------|
| Constant | 10.1983 | 0.4162 | 24.50 | 0.000 |
| Ln (ESDD) | -6.0235 | 0.2599 | -23.18 | 0.000 |

S = 0.330449 R-Sq = 97.8% R-Sq(adj) = 97.6%

PRESS = 1.75952 R-Sq(pred) = 97.07%

Analysis of Variance

| Source | DF | SS | MS | F | P |
|----------------|----|--------|--------|--------|-------|
| Regression | 1 | 58.658 | 58.658 | 537.18 | 0.000 |
| Residual Error | 12 | 1.310 | 0.109 | | |
| Lack of Fit | 3 | 0.644 | 0.215 | 2.90 | 0.094 |
| Pure Error | 9 | 0.667 | 0.074 | | |
| Total | 13 | 59.969 | | | |

Where

SE coef – Standard error coefficient

T – Standard “T” Statistic

P – Probability of testing the significance of null hypothesis

F- Standard “F” statistic

S – Standard deviation

PRESS – Prediction error sum of squares

R² – Residual sum of squares

R² (adj) – Adjusted residual sum of squares

R² – (pred) - Predicted residual sum of squares

DF – Degrees of freedom

SS – Sum of squares

MS – Mean sum of squares

In general a high value of R² (adj), indicates that the model is capable of explaining the variability in a wide range. A high value of R²(pred) indicates the capability in predicting the variability in new observations and is correlated with a low value of PRESS. A high “F” ratio and low “p” value means that the model is highly significant [26 27]. In order to validate the model in the region of extrapolation a data point - ESDD of 0.08 was considered.

*Predicted Values for New Observations at 95% Prediction Interval = (24.49 kV, 26.33 kV)
 From Experiment = 24.5 kV*

Thus the experimentally obtained value is observed to be within the range of 95% prediction limits and thus the model is validated. Figure 4.8 shows the FOV prediction at 95% prediction interval for new silicone rubber where in there are two sections, one is the experimental data from ESDD 0.12 to 0.32 mg/cm² and the other is the projected/validated region from ESDD 0.11 to 0.04 mg/cm² in one side and from 0.35 to 0.45 mg/cm² on the other side. In Figure 4.8 CI represents confidence interval, PI the prediction interval, LL the lower limit of PI and UL the upper limit of PI. From Figure 4.8 an estimate of the range of FOV for very low values of ESDD where actual experiments are not possible can be obtained.

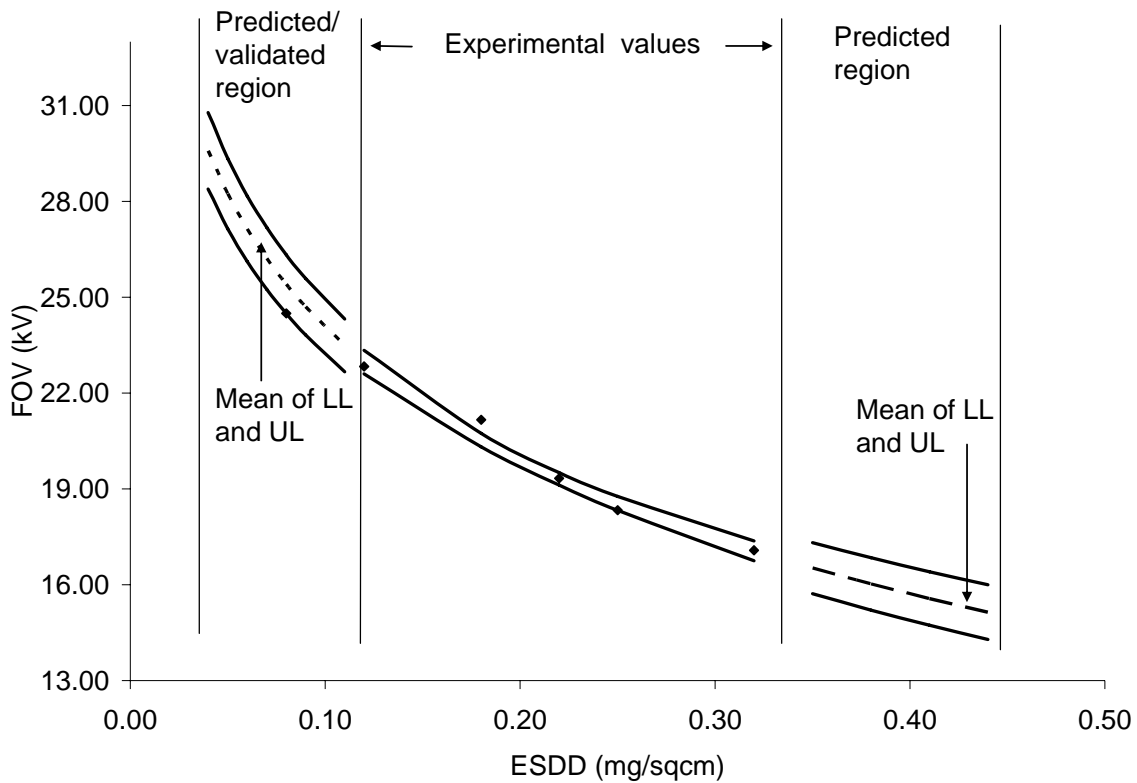


Figure 4.8: FOV prediction curve at 95% Prediction interval for new silicone rubber

b) Aged silicone rubber housing

Regression Analysis: FOV versus ln (ESDD)

The regression equation is
FOV = 7.33 - 6.52 ln (ESDD)

| Predictor | Coef | SE Coef | T | P |
|-----------|---------|---------|--------|-------|
| Constant | 7.3294 | 0.3372 | 21.73 | 0.000 |
| ln (ESDD) | -6.5165 | 0.2123 | -30.69 | 0.000 |

S = 0.267489 R-Sq = 97.7% R-Sq(adj) = 97.6%
PRESS = 1.87678 R-Sq(pred) = 97.28%

Analysis of Variance

| Source | DF | SS | MS | F | P |
|----------------|----|--------|--------|--------|-------|
| Regression | 1 | 67.384 | 67.384 | 941.77 | 0.000 |
| Residual Error | 22 | 1.574 | 0.072 | | |
| Lack of Fit | 6 | 0.407 | 0.068 | 0.93 | 0.499 |
| Pure Error | 16 | 1.167 | 0.073 | | |
| Total | 23 | 68.958 | | | |

Figure 4.9 shows the FOV prediction at 95% prediction interval for aged silicone rubber, the experimental data is from ESDD 0.15 to 0.32 mg/cm² and the projected/validated region is from ESDD 0.13 to 0.05 mg/cm² in one side and from 0.33 to 0.44 mg/cm² on other side. In order to validate the model in the region of extrapolation a data point - ESDD of 0.13 was considered.

Predicted Values for New Observations at 95% Prediction Interval = (20.02 kV, 21.23 kV)
From Experiment = 20.83 kV

Thus the experimentally obtained value is observed to be within the range of 95% prediction limits and thus the model is validated.

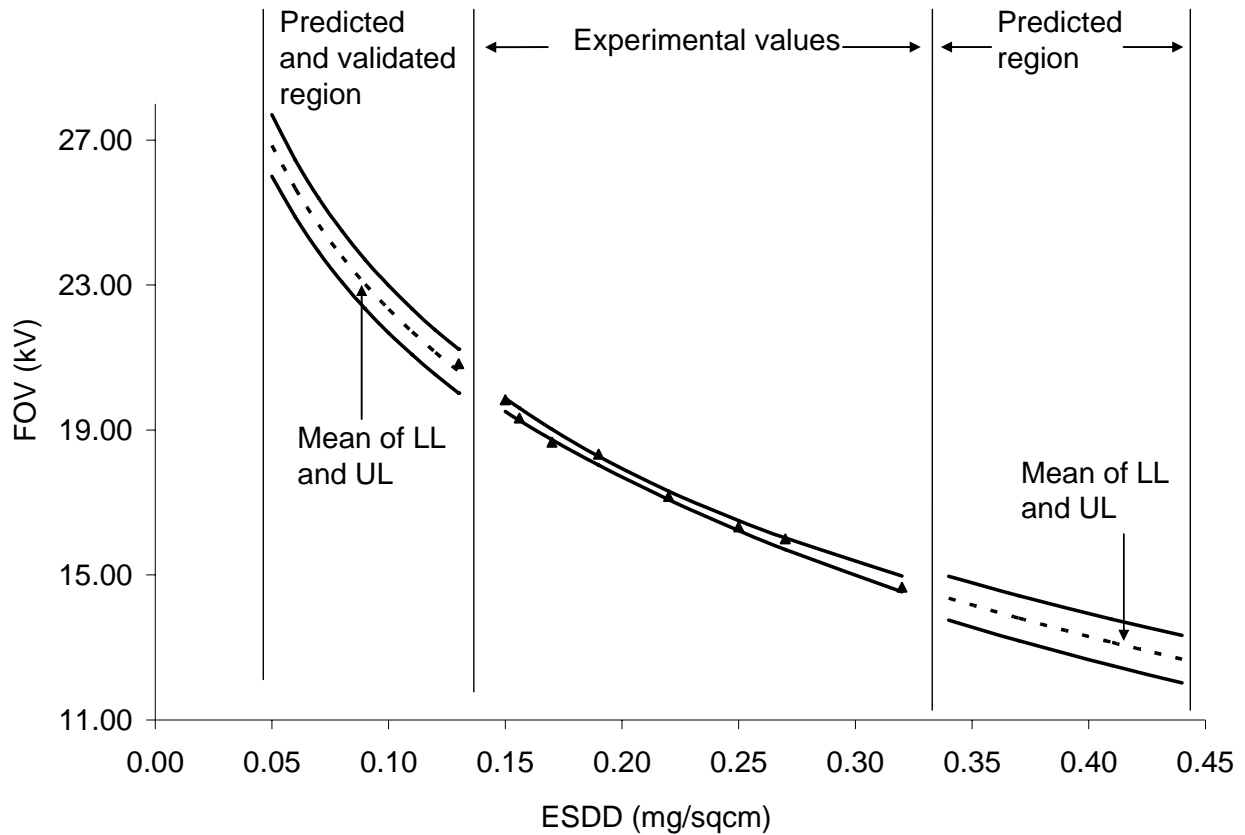


Figure 4.9: FOV prediction curve at 95% Prediction interval for aged silicone rubber

c) Aged EPDM housing material

Regression Analysis: FOV versus ln(ESDD)

The regression equation is
 $FOV = - 9.90 \ln(ESDD)$

| Predictor | Coef | SE Coef | T | P |
|------------|----------|---------|---------|-------|
| Noconstant | | | | |
| ln(ESDD) | -9.89945 | 0.06946 | -142.51 | 0.000 |

S = 0.367873
 PRESS = 2.18039

Analysis of Variance

| Source | DF | SS | MS | F | P |
|----------------|----|--------|--------|----------|-------|
| Regression | 1 | 2748.6 | 2748.6 | 20310.33 | 0.000 |
| Residual Error | 14 | 1.9 | 0.1 | | |
| Lack of Fit | 4 | 1.1 | 0.3 | 3.18 | 0.063 |
| Pure Error | 10 | 0.8 | 0.1 | | |
| Total | 15 | 2750.5 | | | |

Figure 4.10 shows the FOV prediction at 95% prediction interval for aged EPDM, the experimental data is from ESDD 0.20 to 0.34 mg/cm² and the projected/validated region is from ESDD 0.18 to 0.13 mg/cm² in one side and from 0.36 to 0.44 mg/cm² on the other side. In order to validate the model in the region of extrapolation a data point - ESDD of 0.18 was considered.

Predicted Values for New Observations at 95% Prediction Interval = (16.15 kV, 17.80 kV)
From Experiment = 16.67 kV

Thus the experimentally obtained value is observed to be within the range of 95% prediction limits and thus the model is validated

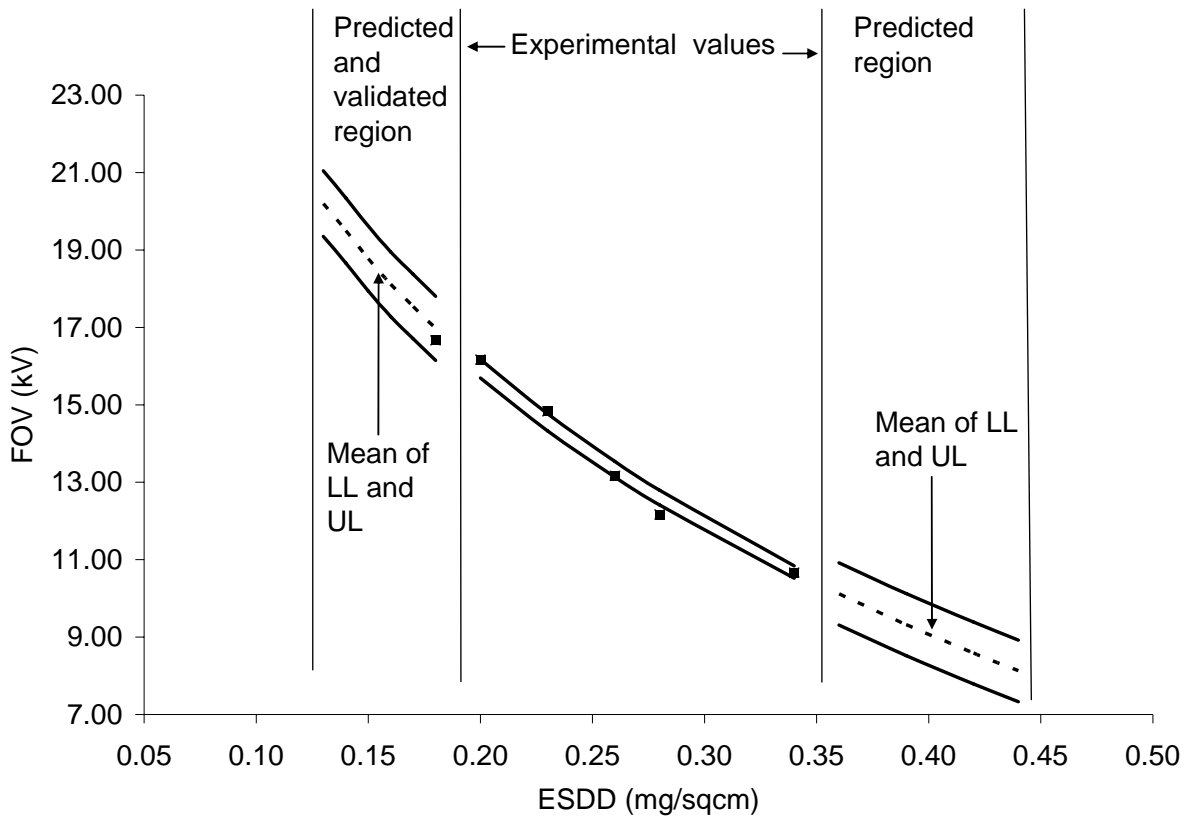


Figure 4.10: FOV prediction curve at 95% Prediction interval for aged EPDM

d) Porcelain

Regression Analysis: FOV versus ln(ESDD)

The regression equation is
FOV = - 7.84 ln(ESDD)

| Predictor | Coef | SE Coef | T | P |
|------------|----------|---------|---------|-------|
| Noconstant | | | | |
| ln(ESDD) | -7.84361 | 0.06801 | -115.33 | 0.000 |

S = 0.320742
PRESS = 1.01321

Analysis of Variance

| Source | DF | SS | MS | F | P |
|----------------|----|--------|--------|----------|-------|
| Regression | 1 | 1368.4 | 1368.4 | 13301.75 | 0.000 |
| Residual Error | 8 | 0.8 | 0.1 | | |
| Lack of Fit | 2 | 0.3 | 0.2 | 1.94 | 0.224 |
| Pure Error | 6 | 0.5 | 0.1 | | |
| Total | 9 | 1369.3 | | | |

Figure 4.11 shows the FOV prediction at 95% prediction interval for porcelain, the experimental data is from ESDD 0.12 to 0.32 mg/cm² and the other is the projected region from ESDD 0.11 to 0.05 mg/cm² and in other side from 0.35 to 0.45 mg/cm².

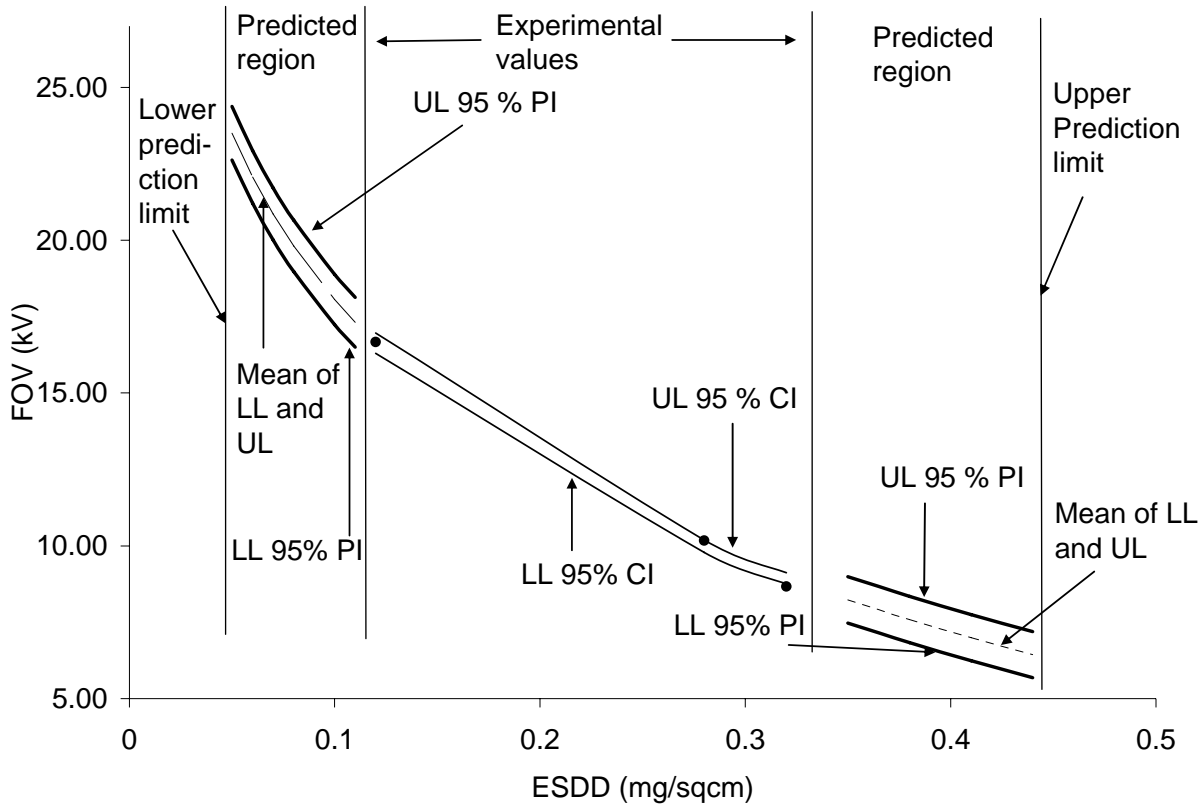


Figure 4.11: FOV prediction curve at 95% Prediction interval for PORCELAIN

4.5 DEVELOPMENT OF A MODEL TO PREDICT FOV BASED ON SURFACE RESISTANCE MEASUREMENT FOR NON-CERAMIC INSULATORS

As mentioned earlier, measurement of the surface resistance can be considered an effective way to analyze the condition of the insulators. The surface resistance of aged silicone rubber and EPDM was measured for different levels of ESDD. From Figure 4.12 it can be observed that for the same ESDD the surface resistance values are much lower for field aged EPDM than field aged silicone rubber and this is due to the hydrophobic property of silicone rubber. The hydrophilic nature of the EPDM can be attributed to the increase in surface energy resulting from chemical degradation. For silicone rubber the dynamics of the hydrophobic surface results in a much higher value of surface resistance than EPDM. The formation of a thick layer of water on the surface of EPDM is much different than that of silicone rubber. All these factors attribute to the difference of surface resistance values for silicone rubber and EPDM [28, 29, 32]. A comparison of experimental results of surface resistance for a constant ESDD is shown in Figure 4.13 for field-aged silicone rubber with and without recovery, new and field aged EPDM and porcelain. The data in Figures 4.12 and 4.13 illustrate the role played by the silicone rubber material towards improving the contamination performance, as the surface resistance is always higher than that of EPDM and porcelain. The actual values that were obtained for surface resistance for different values of ESDD and the corresponding FOV have also been tabulated in Table 6.5 in Appendix A.

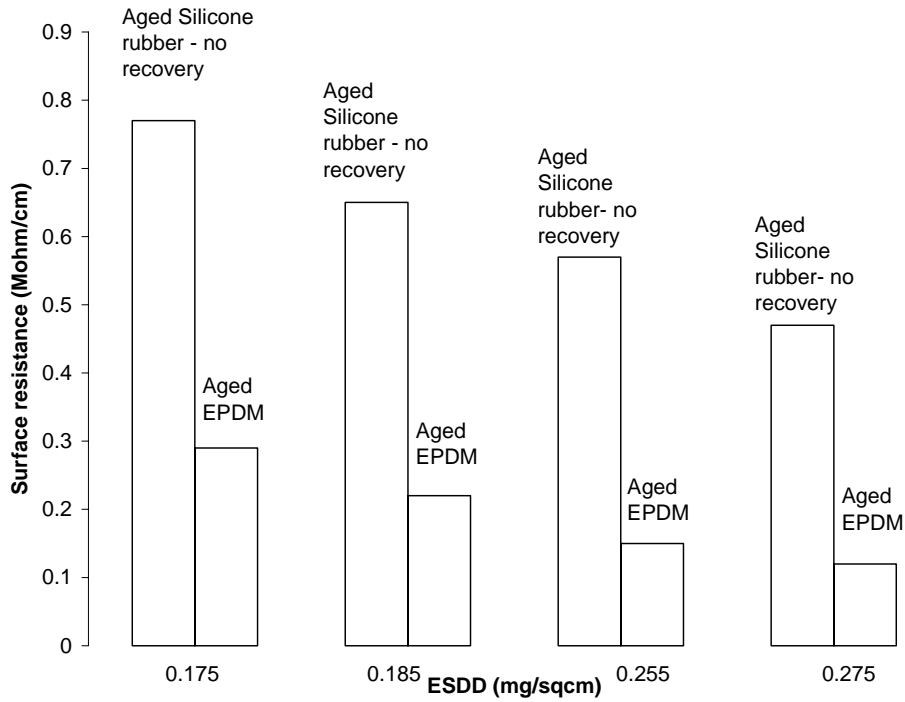


Figure 4.12: Comparison of experimental results of surface resistance vs. ESDD for aged silicone rubber and aged EPDM

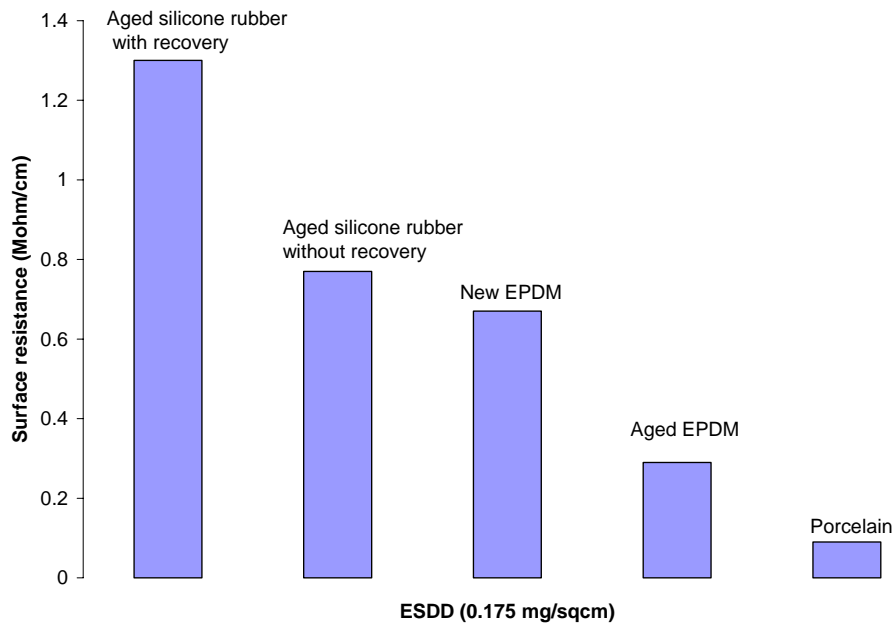


Figure 4.13: Comparison of experimental results of surface resistance for a constant ESDD for aged silicone rubber with and without recovery, aged EPDM and porcelain

Similar to the model that was developed earlier for ESDD and FOV (aged silicone rubber), a regression model was developed for surface resistance and FOV for aged EPDM. As earlier the validity of the assumptions were checked. The regression model for aged EPDM is valid as all the assumptions were satisfied [26, 27].

a) Aged EPDM

Regression analysis approach

Regression Analysis: FOV versus LN (SR)

The regression equation is
 $FOV = 26.2 + 6.73 \text{ LN}(\text{SR})$

| Predictor | Coef | SE Coef | T | P |
|-----------|---------|---------|-------|-------|
| Constant | 26.2482 | 0.9064 | 28.96 | 0.000 |
| LN(SR) | 6.7332 | 0.4871 | 13.82 | 0.000 |

S = 0.365765 R-Sq = 96.5% R-Sq(adj) = 96.0%
 PRESS = 1.49460 R-Sq(pred) = 94.36%

Analysis of Variance

| Source | DF | SS | MS | F | P |
|----------------|----|--------|--------|--------|-------|
| Regression | 1 | 25.564 | 25.564 | 191.08 | 0.000 |
| Residual Error | 7 | 0.936 | 0.134 | | |
| Lack of Fit | 1 | 0.436 | 0.436 | 5.24 | 0.062 |
| Pure Error | 6 | 0.500 | 0.083 | | |
| Total | 8 | 26.500 | | | |

Figure 4.14 shows the FOV prediction curve at 95% Prediction interval for aged EPDM based on surface resistance.

Predicted Values for New Observations at 95% Prediction Interval = (8.92 kV, 11.15 kV)
From Experiment = 10.67 kV

Thus the experimentally obtained value is observed to be within the range of 95% prediction limits and thus the model is validated

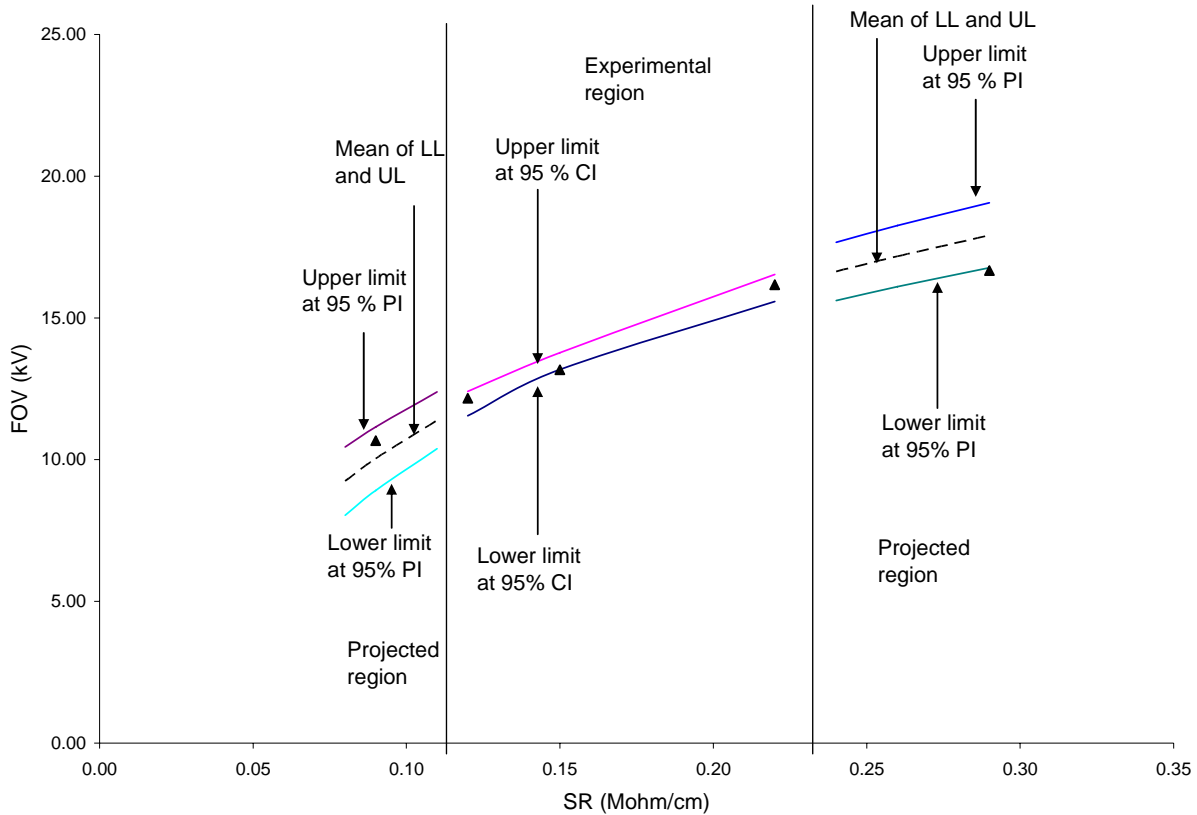


Figure 4.14: FOV prediction curve at 95% prediction interval for aged EPDM based on surface resistance

b) Alternative approach based on critical value of surface resistance for EPDM

Figure 4.15 shows the EPDM samples evaluated for estimating critical surface resistance. The critical value of surface resistance can be defined as the value until which the insulator can be termed to be safe to operate in line. All the samples tested were installed around 1981. The service area can be characterized as fairly clean, typically level 1 as per the IEC 60815. Porcelain insulators with a specific creepage distance of 16 mm/kV have worked satisfactorily in such locations. The EPDM insulators used had a similar value. Three of the insulators flashed over after about 25 years in service. Two insulators from an adjoining structure that had not flashed over were removed and provided as a reference. There are many more of such insulators still in service and it is important to know if these have approached their end of useful life



(a) (b)

Figure 4.15: Insulators evaluated a) severe flashover marks b) No flashover marks

Figure 4.15 shows a flashed insulator along with a sample that did not flashover. These insulators had a leakage distance of 223 cm and a total of 19 sheds of alternating diameter. There was mild chalking on the insulator surface. All insulators had lost their hydrophobicity, and mild chalking was evident. There was no deposition of contamination that one might suspect that the flashover was due to airborne contaminants. Table 4.7 summarizes the visual observations of the samples evaluated. ESDD was measured at 5 random places in each of the insulators. The area chosen for ESDD measurement was small and did not affect further tests on the insulator. Table 4.8 shows the obtained values. IEC 60815 classifies these values as levels 1-2, very light to moderate pollution

Table 4.7. Visual observations of the samples evaluated

| Insulator | Comments |
|------------------|--|
| 1 | No Flashover, no visible signs of contamination except for chalking |
| 2 | Same as above |
| 3 | Flashed over, few sheds discolored on one side, power arc damage on end-fittings |
| 4 | Flashed over, all sheds discolored on one side, power arc damage on end-fittings |
| 5 | Same as above |

Table 4.8. ESDD values in mg/cm² for EPDM insulators

| Location | Insulator | | | | |
|----------------|--------------|--------------|--------------|--------------|--------------|
| | 1 | 2 | 3 | 4 | 5 |
| 1 | 0.008 | 0.008 | 0.104 | 0.044 | 0.018 |
| 2 | 0.014 | 0.019 | 0.073 | 0.067 | 0.100 |
| 3 | 0.032 | 0.031 | 0.109 | 0.079 | 0.074 |
| 4 | 0.026 | 0.060 | 0.050 | 0.089 | 0.064 |
| 5 | 0.032 | 0.064 | 0.076 | 0.013 | 0.074 |
| Average | 0.023 | 0.037 | 0.082 | 0.058 | 0.066 |

A Matlab program was written to predict the FOV. Table 4.9 shows the predicted flashover voltage for various insulators for the average level of ESDD shown in Table 4.8. It can be observed that the flashover voltage is much higher than the nominal operating voltage of 80 kV. Thus there should have been no flashover in service. In reality we had observed flashover which contradicts the prediction. In order to account for this the surface resistance of the insulators was evaluated by the same method as explained earlier. Figure 4.16 shows the measured surface resistance values. No significant difference was observed in the values of surface resistance along the insulator. The leakage current waveforms of some samples are shown in Figures 4.17 and 4.18.

Table 4.9. Matlab based simulation results

| Insulator | 1 | 2 | 3 | 4 | 5 |
|-----------|-------|-------|------|-------|-------|
| FOV (kV) | 145.6 | 124.4 | 95.6 | 107.2 | 102.7 |

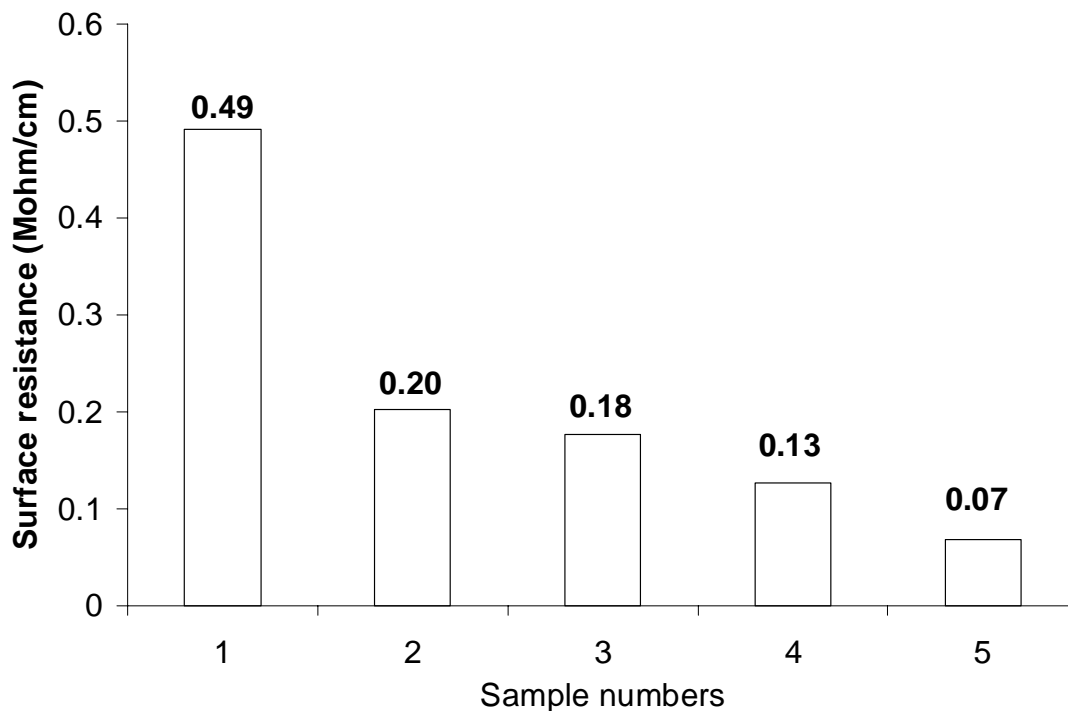


Figure 4.16: Measured surface resistance values of samples 1-5.

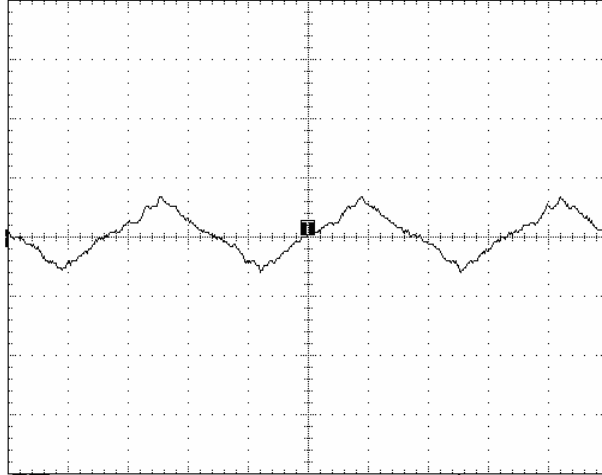


Figure 4.17: Sample (1) tested at 2.0 kV – no discharge (voltage drop = 167 mV)

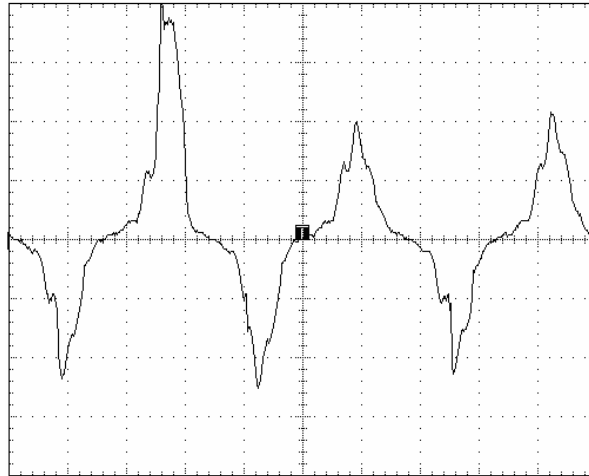


Figure 4.18: Sample (4) tested at 1.5 kV– severe discharge (voltage drop = 478 mV)

In the model presented here, the average value of surface resistance is taken as R_p and simulations are done based on this value. The flow chart of the simulation is given in Figure 4.19.

The model is independent of ESDD. Other parameters like resistance of arc, length of arc and voltage are initialized. After the computation of current and resistance per unit, E_p and E_{arc} are calculated. The electric field of the pollution layer should be greater than field at the tip of the arc for the arc propagation. Flashover is assumed to occur when about 2/3 of the insulator length is bridged by the arc.

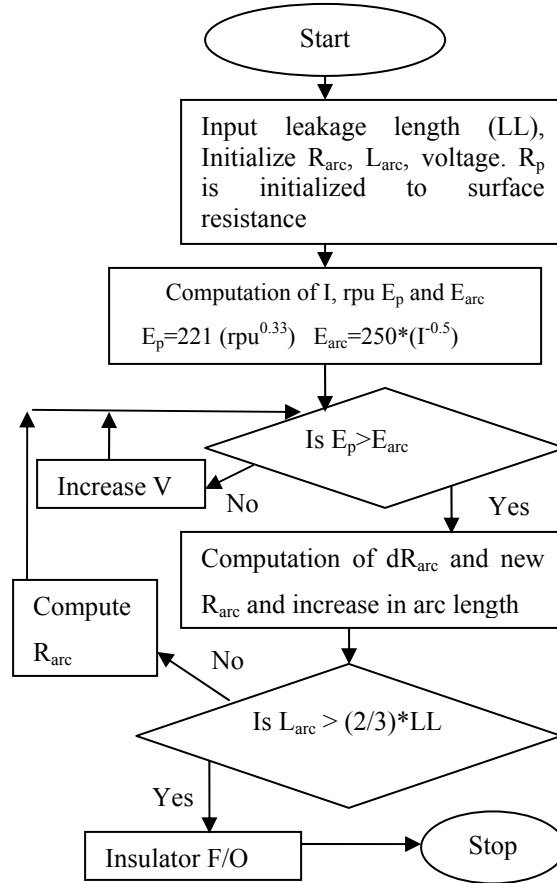


Figure 4.19: Flow chart of proposed simulation model

Table 4.10 shows calculated flashover voltage for the average value of surface resistance determined experimentally on each insulator. Considering that the nominal operating voltage of these 138 kV rated insulators is 80 kV line to ground, it is clear that insulators 4 and 5 have a high possibility of flashover, insulators 2 and 3 are very close to flashover.

The results shown in Figure 4.16 and Table 4.10 suggest that a surface resistance value of about 300 kΩ/cm could be considered as a critical value below which there is a high risk of flashover. Since these insulators did not show any significant variation in surface resistance along the insulator length, it is reasonable to assume that the aging is more determined by weathering than by nonlinear electric stress distribution. An additional merit of the surface resistance approach is that the procedure can be adapted for field use.

Table 4.10. Simulation results based on surface resistance

| Sample | 1 | 2 | 3 | 4 | 5 |
|----------|-------|------|------|------|------|
| FOV (kV) | 112.6 | 83.4 | 80.4 | 72.2 | 58.6 |

Insulator flashover in the field is dependent on many factors such as wind, the presence of wet and dry areas with the protected surfaces generally being hard to wet, deviations from the

nominal voltage due to loading, etc. Theoretical models can only help determine how close they are to flashover assuming ideal wetting conditions. From this perspective, the model based on surface resistance is obviously far superior to ESDD based models developed for porcelain insulators.

c) Generalized approach for FOV prediction based on measurement of surface resistance and leakage distance.

Based on the measurement of flashover voltage for different leakage lengths and the corresponding values of surface resistance for different insulators a plot which combines all these aspects is shown in Figure 4.20.

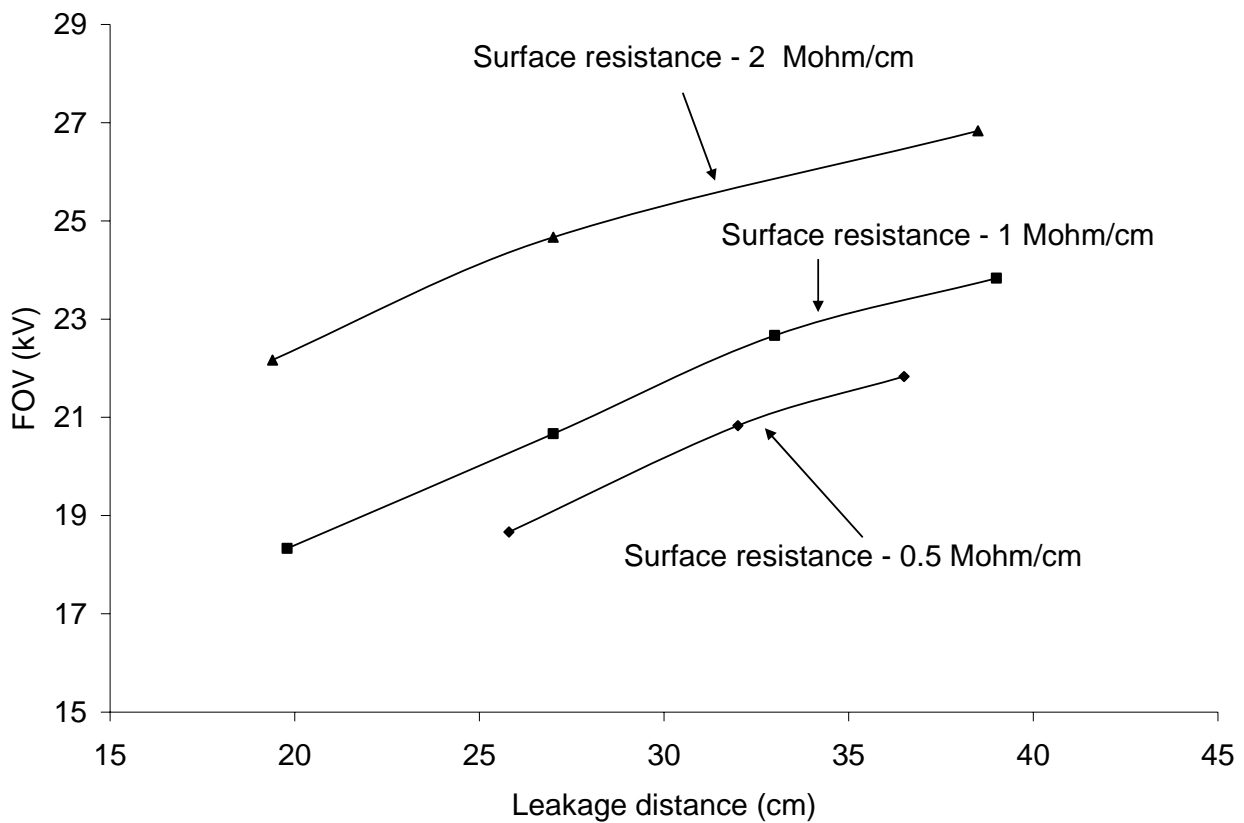


Figure 4.20: FOV for different surface resistance vs leakage distance

4.6 DEVELOPMENT OF A MODEL TO PREDICT FOV BASED ON LEAKAGE DISTANCE

It is known that the FOV will increase with leakage distance. However the improvement obtained in the FOV for various materials for the same ESDD and leakage distance is not known. This information is useful to determine insulator dimensions as a function of material type. The

ESDD level selected for comparison was 0.13 mg/cm^2 , which represents heavy contamination. Figure 4.21 shows the graph that compares silicone rubber and EPDM performance. The following can be inferred from Figure 4.21,

- When compared to EPDM for the same leakage distance, contamination severity (ESDD) and field aging, the use of silicone rubber provides up to a 30% improvement in FOV if the surface hydrophobicity has recovered. If there is no hydrophobicity recovery, the improvement is about 10%.
- New silicone rubber housing is capable of providing the same FOV as a new EPDM with 74% less leakage distance. With aging of the silicone rubber material and complete loss of hydrophobicity, the same FOV is obtained with a reduction of 20% when compared to the aged EPDM material.

In the field, complete loss of hydrophobicity is rare. So the average improvement obtained in the contamination performance is somewhere in between the two extremes mentioned above. In order to predict the FOV for different leakage lengths a regression model was fitted and checked for the validity of assumptions. The regression model was validated by experiment at a point outside the region of the model with a high prediction interval of 95%.

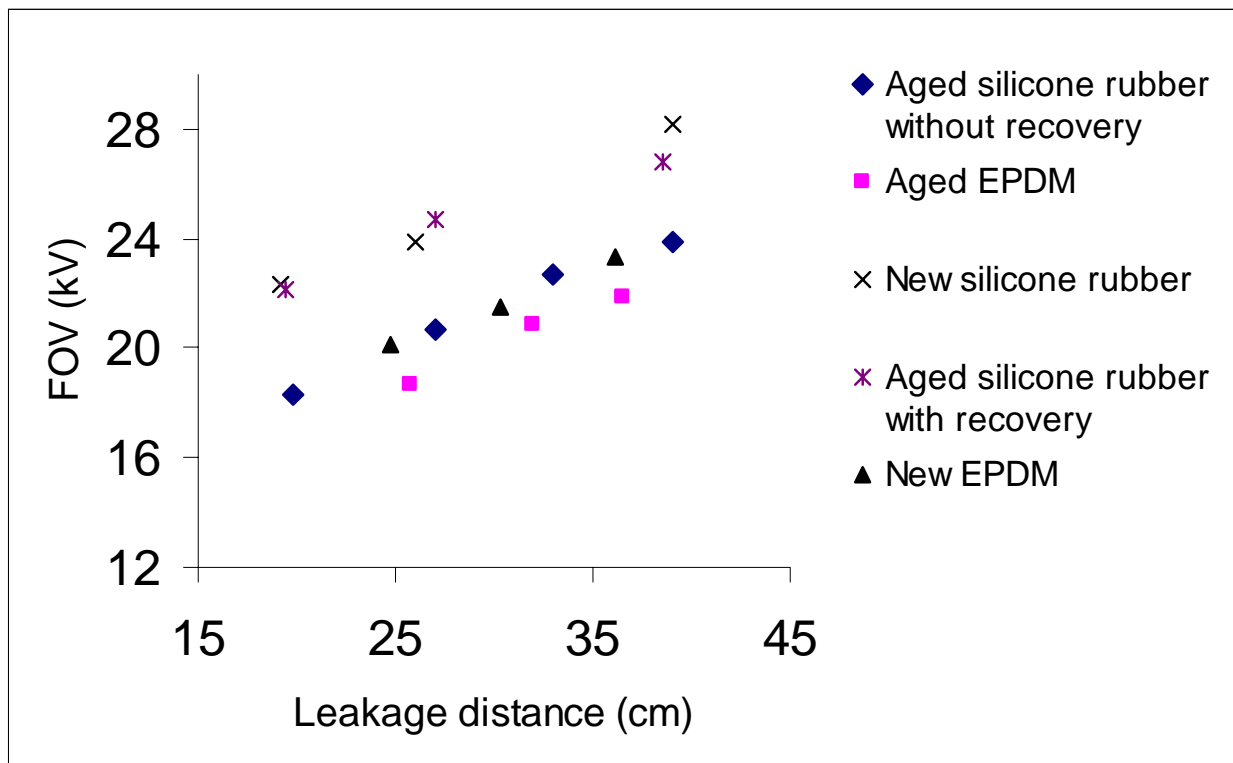


Figure 4.21: Variation of FOV with leakage distance for different materials

a) Aged EPDM

Regression Analysis: FOV versus LD

The regression equation is
 $FOV = - 11.2 + 9.22 \ln(LD)$

| Predictor | Coef | SE Coef | T | P |
|-----------|---------|---------|-------|-------|
| Constant | -11.249 | 2.307 | -4.88 | 0.002 |
| ln (LD) | 9.2190 | 0.6705 | 13.75 | 0.000 |

S = 0.287658 R-Sq = 96.4% R-Sq(adj) = 95.9%
PRESS = 0.967736 R-Sq(pred) = 94.03%

Analysis of Variance

| Source | DF | SS | MS | F | P |
|----------------|----|--------|--------|--------|-------|
| Regression | 1 | 15.643 | 15.643 | 189.05 | 0.000 |
| Residual Error | 7 | 0.579 | 0.083 | | |
| Lack of Fit | 1 | 0.079 | 0.079 | 0.95 | 0.367 |
| Pure Error | 6 | 0.500 | 0.083 | | |
| Total | 8 | 16.222 | | | |

Figure 4.22 shows the FOV prediction curve at 95% Prediction interval for aged EPDM based on leakage distance.

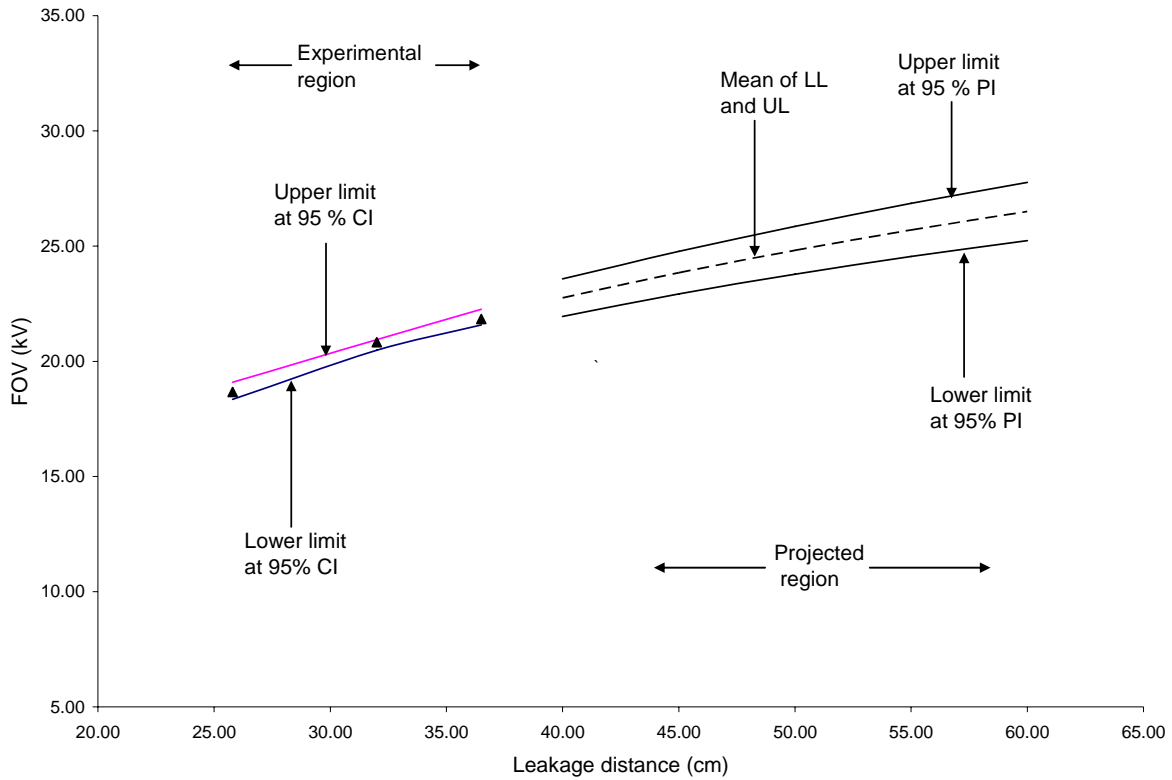


Figure 4.22: FOV prediction curve at 95% Prediction interval for aged EPDM based on leakage distance

b) Aged silicone rubber – no recovery / New EPDM

The regression equation is
 $FOV = - 6.83 + 8.40 \ln (LD)$

| Predictor | Coef | SE Coef | T | P |
|-----------|--------|---------|-------|-------|
| Constant | -6.826 | 1.608 | -4.24 | 0.004 |
| Ln (LD) | 8.4010 | 0.4924 | 17.06 | 0.000 |

S = 0.310435 R-Sq = 97.7% R-Sq(adj) = 97.3%
 PRESS = 1.10855 R-Sq(pred) = 96.14%

Analysis of Variance

| Source | DF | SS | MS | F | P |
|----------------|----|--------|--------|--------|-------|
| Regression | 1 | 28.048 | 28.048 | 291.04 | 0.000 |
| Residual Error | 7 | 0.675 | 0.096 | | |
| Lack of Fit | 1 | 0.175 | 0.175 | 2.10 | 0.198 |
| Pure Error | 6 | 0.500 | 0.083 | | |
| Total | 8 | 28.722 | | | |

Figure 4.23 shows the FOV prediction curve at 95% Prediction interval for aged silicone rubber no recovery / New EPDM based on leakage distance

Predicted Values for New Observations at 95% Prediction Interval = (23.05 kV, 24.86 kV)
From Experiment = 23.67 kV

Thus the experimentally obtained value is observed to be within the range of 95% prediction limits and thus the model is validated.

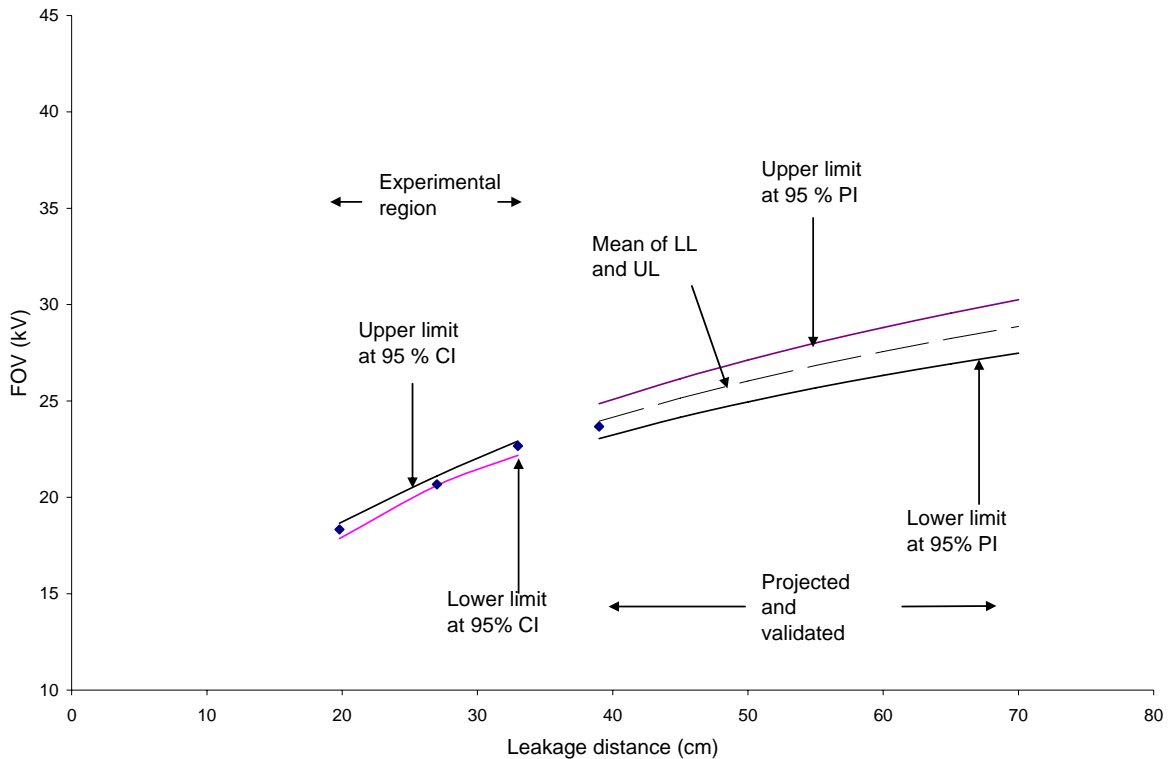


Figure 4.23: FOV prediction curve at 95% Prediction interval for aged silicone rubber no recovery / new EPDM based on leakage distance

4.7 STUDY OF RECOVERY ASPECTS OF SILICONE RUBBER AND EPDM VIA SURFACE RESISTANCE MEASUREMENTS

The term recovery can be defined in terms of resting time as the time interval between the application of contamination and the start of the test. In this work the samples were subjected to open air atmosphere under natural environmental conditions. The recovery period was typically for three days on the roof of the laboratory where maximum day time temperatures of 45°C are common. The surface resistance measurement was done on aged silicone rubber samples, as well as aged EPDM samples with and without recovery for the same ESDD of 0.175 mg/cm². Figures 4.24 and 4.25 show the results obtained for two different EPDM samples. Figures 4.26 and 4.27 show the results obtained for two different silicone rubber samples. From Figures 4.24, 4.25 it is

quite evident that the recovery exerts little influence on the electrical performance of EPDM insulators due to material characteristic and hydrophilic nature. EPDM has a tendency to absorb moisture. From Figures 4.26, 4.27 it is evident the recovery is shown to dramatically improve the electrical performance of silicone rubber insulators.

Experimental evidence has indicated that the recovery process of hydrophobicity in silicone rubber insulators is a progressive superposition of (low molecular weight silicone polymer) silicone oil layers with time that beads up water droplets. After the sample has been contaminated the differences in concentration gradients in the bulk of the material and contaminated surface triggers the silicone oil diffusion process. This transfer of silicone oil to certain areas of the contaminated layer might prevent a complete dissolution of conductive material in wet conditions. Hence, there is a considerable decrease in contamination layer thickness. Therefore, the net effect of recovery can be viewed as a process in which there is a gradual reduction of effective contamination layer thickness. This reduction of the effective contamination layer can explain to some extent how a seemingly wettable silicone rubber insulator is able to withstand higher FOV [27, 29, 30, 31].

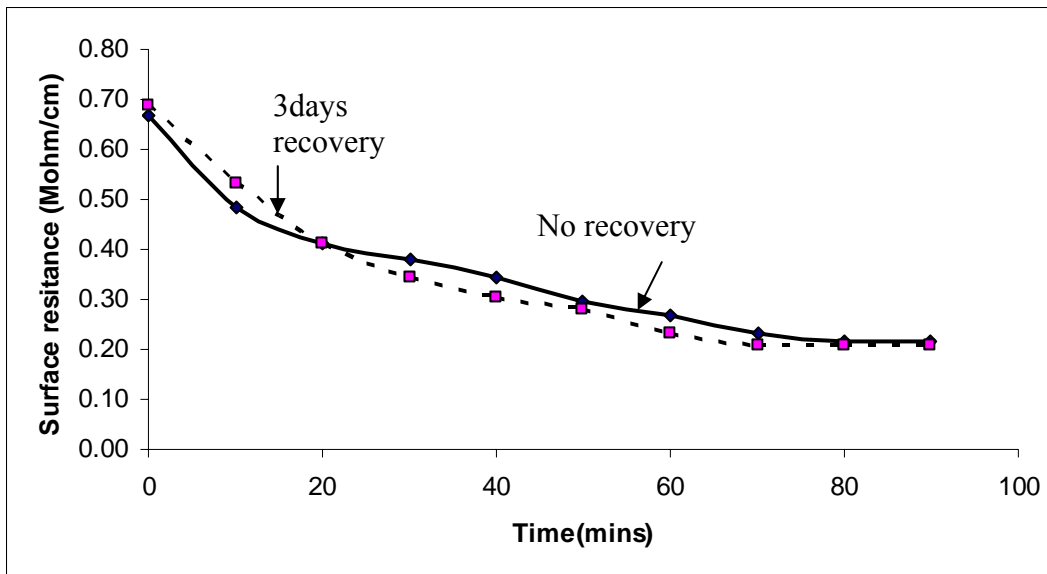


Figure 4.24: Variation of Surface Resistance (SR) vs time for aged EPDM sample “A” with and without recovery

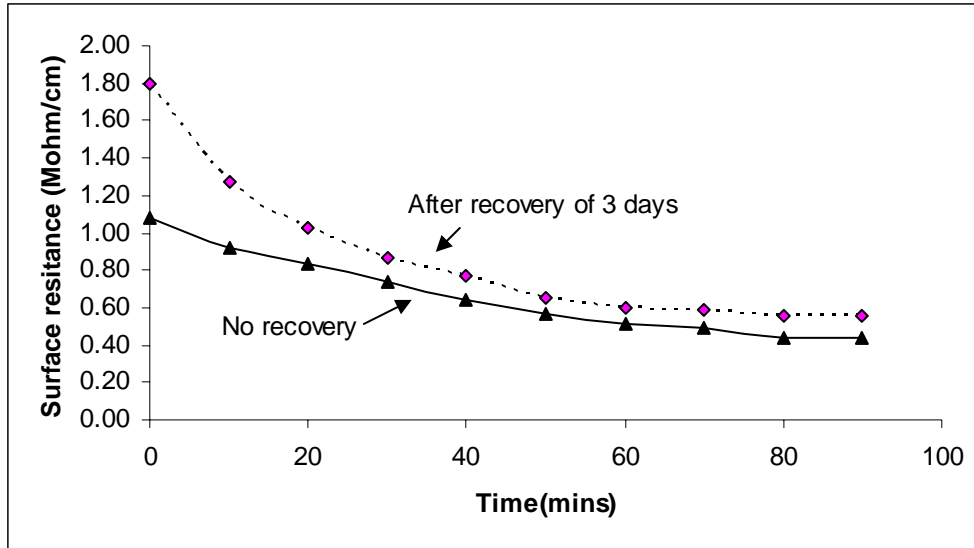


Figure 4.25: Variation of Surface Resistance (SR) vs time for aged EPDM sample "B" with and without recovery

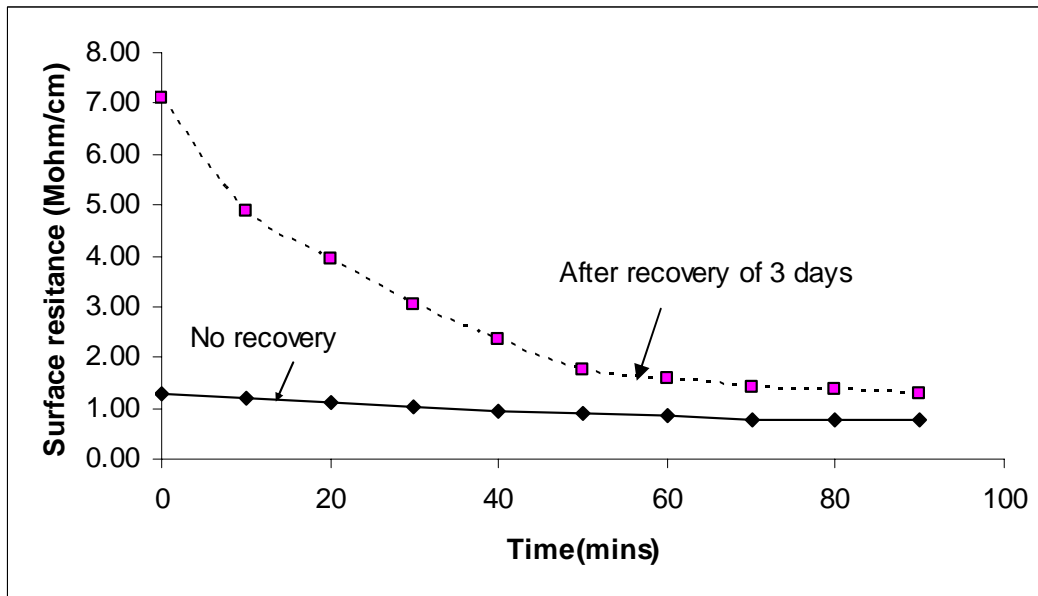


Figure 4.26: Variation of Surface Resistance (SR) vs time for aged Silicone rubber sample "A" with and without recovery

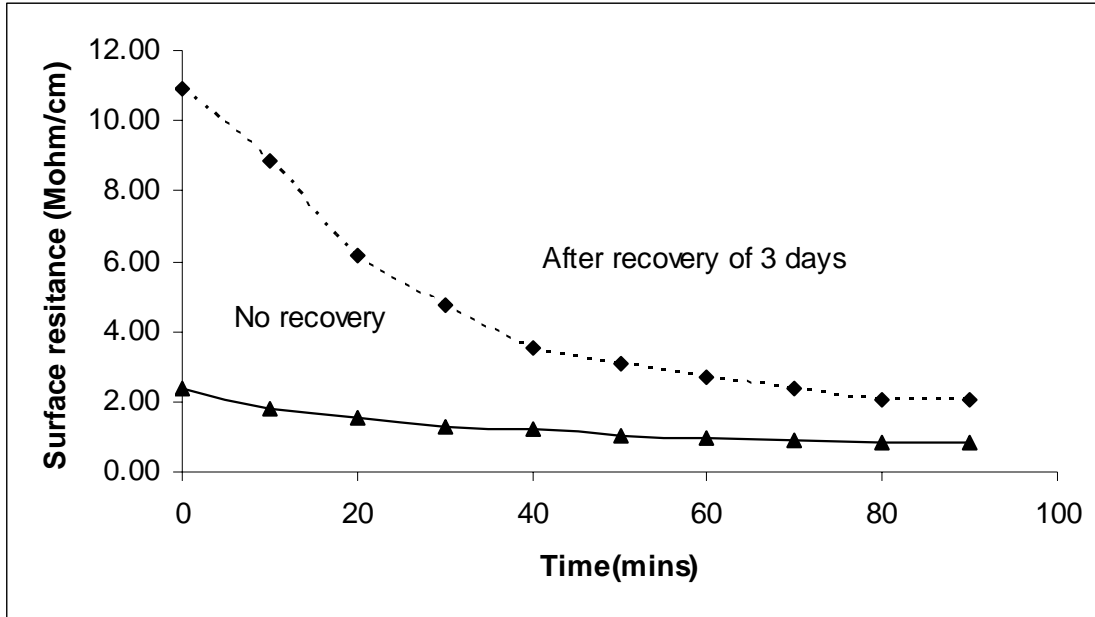


Figure 4.27: Variation of Surface Resistance (SR) vs time for aged Silicone rubber sample “B” with and without recovery

4.8 THEORETICAL MODEL FOR NCI

A dynamic model described in [10] was used as the basis for the model proposed in this paper. This model takes into account the profile of the insulator and the dynamic change in the arc resistance as it traverses along the leakage length of the insulator. In order to determine the reignition constant that could be used for silicone rubber, electric-field simulations were performed using “*Electro*” software [33]. This package offers two choices - rotationally symmetric or two dimensional modeling. The latter was chosen for this work as the geometry modeled is a flat plate. The computation error was less than 5% (determined by the difference of the integral of the axial electric field from the applied voltage). Two identical slabs of dimension 20 cm x 20 cm with parallel plate electrodes were considered as shown in Figures 4.28 and 4.29. The flow of water is modeled as a triangle. As porcelain surface is wettable, the water path is assumed to have a large base when compared to silicone rubber where the water path is approximated as a filament. A series of simulations were performed by varying the area of the water channel and the distance of the tip of the channel from the HV end. The electric field at the tip of the water channel was calculated for various combinations of area (water channel) and distance (tip from HV).

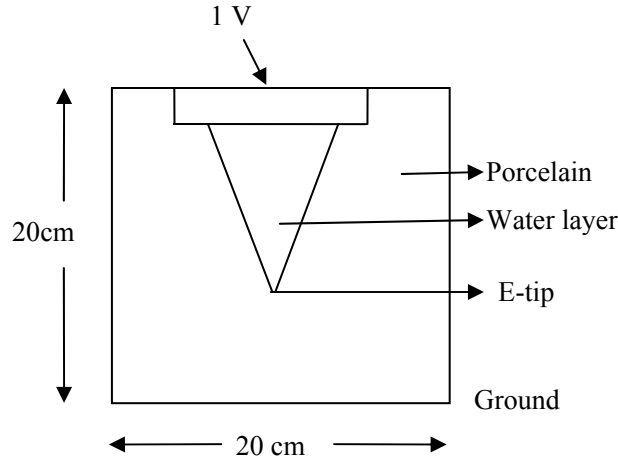


Figure 4.28: Simulation model considered for porcelain

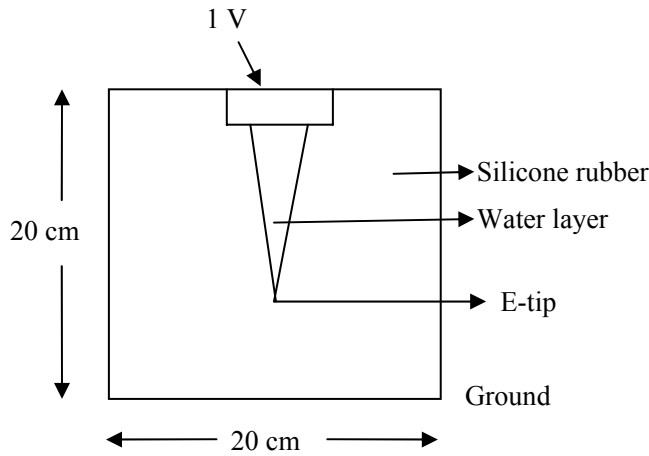


Figure 4.29: Simulation model considered for silicone rubber

$$E_{field} (porcelain) = K1*(A*D) + C1 \quad (4)$$

$$E_{field} (silicone) = K2*(A*D) + C2 \quad (5)$$

Here K1, C1, (for porcelain) and, K2, C2 (for silicone) are numerical constants obtained from a linear regression fit (statistical) of the electric field data to the product of area and distance. The ratio of K2/K1 is 5.8. The electric field simulation results are given in Tables 4.11 and 4.12. The statistical results obtained using regression analyses are given after Table 4.12. The values of constants derived from the simulations are given in Table 4.13. It is to be expected that the aged silicone rubber which shows better flashover performance than porcelain will have the reignition constant value higher than porcelain and lower than new silicone rubber. For aged silicone rubber that has no recovery and behaves like a new EPDM material, and for aged EPDM the values of different constants that provide a good fit to experimental data are also given in Table 4.13. The value of constant to be used for silicone rubber samples with varying degree of hydrophobicity recovery is a subject for further research.

Table 4.11. Electric field simulation results for porcelain model

| Area (A) (cm ²) | Distance (D) (cm) | A*D | E-field (V/cm) |
|--------------------------------|----------------------|-------|-------------------|
| 5.22 | 0.78 | 4.08 | 0.061 |
| 11.00 | 1.64 | 18.08 | 0.057 |
| 14.25 | 2.24 | 31.88 | 0.053 |
| 14.97 | 2.24 | 33.49 | 0.052 |
| 22.19 | 3.32 | 73.59 | 0.044 |

Table 4.12. Electric field simulation results for silicone rubber model

| Area (A1) (cm ²) | Distance (D1) (cm) | A1*D1 | E-field 1 (V/cm) |
|---------------------------------|-----------------------|--------|---------------------|
| 10.74 | 8.40 | 90.20 | 0.357 |
| 12.25 | 9.57 | 117.18 | 0.306 |
| 13.26 | 10.36 | 137.43 | 0.278 |
| 13.86 | 10.83 | 150.07 | 0.264 |
| 14.76 | 11.54 | 170.33 | 0.244 |

Regression Analysis: Efield versus A*D (Porcelain model)

The regression equation is

$$E_{\text{field}} = 0.0612 - 0.000242 A * D$$

| Predictor | Coef | SE Coef | T | P |
|-----------|-------------|------------|--------|-------|
| Constant | 0.0612063 | 0.0006914 | 88.52 | 0.000 |
| A*D | -0.00024225 | 0.00001740 | -13.92 | 0.001 |

S = 0.000904862 R-Sq = 98.5% R-Sq(adj) = 98.0%

PRESS = 0.0000184266 R-Sq(pred) = 88.57%

Analysis of Variance

| Source | DF | SS | MS | F | P |
|----------------|----|------------|------------|--------|-------|
| Regression | 1 | 0.00015874 | 0.00015874 | 193.88 | 0.001 |
| Residual Error | 3 | 0.00000246 | 0.00000082 | | |
| Total | 4 | 0.00016120 | | | |

Regression Analysis: Efield 1 versus A1*D1 (Silicone rubber model)

The regression equation is
 $E_{field\ 1} = 0.477 - 0.00141 A1 \cdot D1$

| Predictor | Coef | SE Coef | T | P |
|-----------|------------|-----------|--------|-------|
| Constant | 0.47724 | 0.01636 | 29.17 | 0.000 |
| A1*D1 | -0.0014089 | 0.0001204 | -11.70 | 0.001 |

S = 0.00741115 R-Sq = 97.9% R-Sq(adj) = 97.1%
 PRESS = 0.000839358 R-Sq(pred) = 89.07%

Analysis of Variance

| Source | DF | SS | MS | F | P |
|----------------|----|-----------|-----------|--------|-------|
| Regression | 1 | 0.0075160 | 0.0075160 | 136.84 | 0.001 |
| Residual Error | 3 | 0.0001648 | 0.0000549 | | |
| Total | 4 | 0.0076808 | | | |

Table 4.13. Recommended values of various constants for different materials

| Material | Reignition constant (<i>N</i>) | Reignition exponent (<i>n</i>) | Arc constant (<i>A</i>) |
|---|----------------------------------|----------------------------------|---------------------------|
| New silicone rubber / Aged silicone rubber with recovery | 340 | 0.5 | 50 |
| Aged silicone rubber with no recovery / New EPDM | 300 | 0.5 | 50 |
| Aged EPDM | 250 | 0.5 | 35 |

4.9 COMPARISON OF EXPERIMENTAL AND SIMULATED RESULTS

In order to compare the simulated and the experimental values, simulations were performed with the developed new set of constants and compared with the experimental results that were obtained for new and aged silicone rubber. Experimental results show that the flashover performance of a new silicone rubber is similar to that of aged silicone rubber that has been allowed to recover its hydrophobicity. Without recovery, this sample behaves like a new EPDM. From Figure 4.30 it can be inferred that the experimental and theoretical simulation matches very closely. This proves the validity of the model proposed.

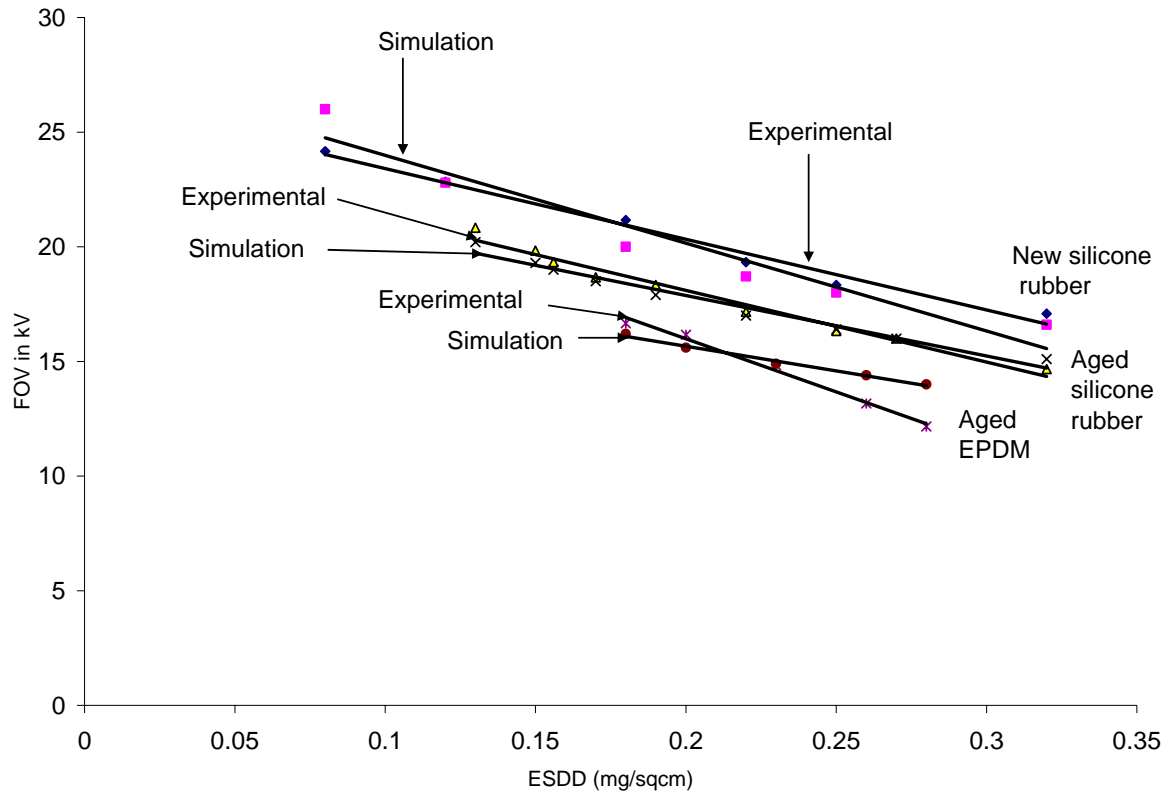


Figure 4.30: Graphical representation to show simulated FOV and experimental FOV for new, aged silicone rubber and aged EPDM

5. CONCLUSIONS AND FUTURE WORK

The conclusions that are drawn from the results obtained are as follows:

- Detailed comparisons of various arcing models were made by Matlab simulations and the values of predicted FOV were observed to be varying in a wide range suggesting the complexity involved in prediction and understanding of flashover.
- Variation of surface resistance of different road salts was studied and the difference in the use of various salts was quantified by simulation in terms of FOV
- The effect of shed bridging was considered and FOV in cases of one, two and three sheds bridging was simulated which indicates the percentage decrease in FOV when sheds are bridged.
- The experiments and simulations on roads salts indicated that the application of liquid salts on the road has an immediate more deleterious effect and will enhance flashover more severely than other salts.
- The effect of water droplets in different sheds was studied for E – field variation which suggested that in any shed the increase in number of water droplets shows an increase in E- field at the tip of the shed and as we move away from the HV end the increase in E- field value at the water droplet/shed junction is significantly lower than observed for the shed which is closest to HV end.
- Development and validation of linear regression models which are capable of predicting with a high prediction interval (95%) FOV based on ESDD for different materials namely
 - New silicone rubber / aged silicone rubber with recovery
 - Aged silicone rubber without recovery / New EPDM
 - Aged EPDM
 - Porcelain
- It can be seen that for the same level of ESDD the FOV for an aged silicone rubber is about 12% less compared to new silicone rubber. The aged EPDM has a FOV of about 16% lower than aged silicone rubber, whereas porcelain has a FOV of about 16% lower than aged EPDM.
- Surface resistance measurement was done for different ESDD for aged silicone rubber without recovery and aged EPDM and thereby the superior performance of silicone material over EPDM was quantified.
- The performance of new silicone rubber / aged silicone rubber with recovery, aged silicone rubber without recovery / new EPDM, aged EPDM and Porcelain were compared in terms of surface resistance value for a constant ESDD.
- Development of linear regression model capable of predicting at (95%) the FOV based on surface resistance for aged EPDM.
- Development and validation of linear regression models which are capable of predicting at (95%) the FOV based on leakage distance for different materials namely
 - Aged silicone rubber without recovery / New EPDM
 - Aged EPDM

- The role of recovery was observed to be important for silicone rubber material as its performance was considerably boosted by recovery whereas in EPDM recovery had little role to play.
- A theoretical model was developed based on simulations using Electro software for non ceramic insulator (silicone rubber) and numeric values of reignition constant and arc constant are proposed for new silicone rubber / aged silicone rubber with recovery, aged silicone rubber without recovery / new EPDM and aged EPDM.
- The theoretical model proposed in this work shows good correlation with experimental results. The model can be used to predict the FOV of silicone rubber and EPDM and also considers the hydrophobic nature of the surface.

The future work in this task includes but is not limited to:

- Develop a instrument to measure surface resistance
- Quantify and justify the relationship between measured surface resistance and actual pollution resistance
- Predict FOV by suitable modeling for partially contaminated insulators

6. REFERENCES

- [1] R. S. Gorur, J. Montesinos, L. Varadadesikan, S. Simmons and M. Shah, "A laboratory test for tracking and erosion resistance of HV outdoor insulation," *IEEE Trans. Dielectrics and Electrical Insulation*, vol. 4, no. 6, pp. 767-774, Dec. 1997.
- [2] J.T. Burnham, P.S. Givens, T.M. Grisham, "High strength polymer post insulators enable economical transmission lines with low environmental impact," Proceedings of the IEEE Power Engineering Society, pp. 494 -503, April 1994.
- [3] R. S. Gorur, S. Sundhara Rajan, and O. G. Amburgey "Contamination performance of polymeric insulating materials used for outdoor insulation applications," *IEEE Trans. Electrical Insulation*, vol. 24, no. 4, pp. 713-716, Aug. 1989.
- [4] E.A. Cherney, "RTV silicone-a high tech solution for a dirty insulator problem," IEEE Electrical Insulation Magazine, vol.11, pp. 8 -14, Nov. 1995.
- [5] <http://www.nzinsulators.co.nz/images/flashover2.jpg>
- [6] http://www.ec.gc.ca/press/000811_b_e.htm
- [7] http://www.riversides.org/review/riversides/low_salt_diet_use.htm
- [8] R. S. Gorur, K. Subramanian, "Use of surface resistance for assessing vulnerability of HV outdoor insulators to contamination flashover," CEIDP, October 2003 pp. 406-409.
- [9] R.S. Gorur, H.M. Schneider, J. Cartwright, Y. Beausajour, K. Kondo, S. Gubanski, R. Hartings, M. Shah, J. McBride, C. de Turreil, Z. Szilagyi, "Surface resistance measurements on non-ceramic insulators," IEEE Transactions on Power Delivery, vol.16, pp. 801 -805, Oct. 2001.
- [10] Sundararajan, R., Gorur, R.S., "Dynamic arc modeling of pollution flashover of insulators under DC voltage", IEEE Transactions on Electrical Insulation, Vol: 28, Issue 2, April 1993, pp. 209-218.
- [11] A. Al-Baghdadi, "The mechanism of flashover of polluted insulation, Ph.D Dissertation, The Victoria university of Manchester, May 1970.
- [12] F. Obenaus, "Contamination flashover and creepage path length," Dtsch. Elektrochnik, vol. 12, pp. 135-136, 1958
- [13] G. Neumarker, "Contamination state and creepage path," Deustsche Akad., Berlin, vol. 1, pp. 352-359, 1959.
- [14] B. Hampton, "Flashover mechanism of polluted insulation," Proceedings of IEEE, vol. 111, pp. 985-990, 1964
- [15] S. Hesketh, "General criterion for the prediction of pollution flashover," Proceedings of IEEE, vol. 114, pp. 531-532, 1967.
- [16] L. Alston, S. Zoledziowsky, "Growth of discharges of polluted insulation," Proceedings of IEEE, vol. 110, pp.1260-1266, 1963.
- [17] F. A. M. Rizk, " A criterion for AC flashover of contaminated insulators" Paper No 71 CP 135-PWR, IEEE Winter Power Meeting, 1971.
- [18] F. A. M. Rizk, "Mathematical models for pollution flashover," Electra No. 78, pp. 71-103, 1981.
- [19] D.C. Jolly, T.C. Cheng and D.M. Otten, " Dynamic theory of discharge growth over contaminated insulator surfaces," Conference Paper No 74-068-3, IEEE PES Winter Power Meeting, 1974.
- [20] Sundararajan, R., "Dynamic arc modeling of pollution flashover of insulators under energized with direct current voltage," Ph.D. Dissertation, Dept of Elec Engg, Arizona State University, USA 1993.

- [21] Rizk, F.A.M.; Kamel, S.I.; “Modelling of HVDC wall bushing flashover in nonuniform rain,” IEEE Transactions on Power Delivery, vol.6, pp. 1650-1652, Oct. 1991.
- [22] H. M. Schneider, A. E. Lux, “Mechanism of HVDC wall bushing flashover in non- uniform rain,” IEEE Transactions on Power Delivery, vol. 6, pp. 448-455, Jan. 1991.
- [23] Gorur, R.S., De La O, A., El-Kishky, H., Chowdhary, M., Mukherjee, H., Sundaram, R., Burnham, J.T, “Sudden flashover of non-ceramic insulators in artificial contamination tests,” IEEE Transactions on Electrical Insulation, Vol: 4, Issue 1, Feb1997, pp. 79-87.
- [24] De la O, A., Gorur, R.S., “Flashover of contaminated non-ceramic outdoor insulators in a wet atmosphere,” IEEE Transactions on Electrical Insulation, Vol: 5, Issue 6, Dec1998, pp. 814-823.
- [25] J. P. Holtzhausen “A critical evaluation of AC pollution flashover models for HV insulators having hydrophilic surfaces,” Ph.D Dissertation, Dept of Elec Engg, University of Stellenbosch, South Africa, November 1997.
- [26] Douglas C Montgomery, “Design and Analysis of Experiments,” 5th edition, John Wiley and Sons Inc.
- [27] D. C. Montgomery, E. A. Peck, G. G. Vining, “Introduction to linear regression analysis,” 3rd edition, New York, John Wiley and Sons, 2001.
- [28] De la O, A “Alternating current flashover behavior of contaminated non-ceramic insulators in a wet atmosphere,” Ph.D Dissertation, Dept of Elec Engg, Arizona State University, USA 1997.
- [29] K. Subramanian “Use of surface resistance for assessing vulnerability of HV outdoor insulators to contamination flashover,” M.S. Thesis, Dept of Elec Engg, Arizona State University, USA 2004
- [30] Gorur, R.S. Chang, J.W, Amburgey, O.G., “Surface hydrophobicity of polymers used for outdoor insulation,” IEEE Transactions on Power Delivery, vol. 5, pp. 1923-1933, 1990.
- [31] Chang, J.W Gorur, R.S. “Surface recovery of silicone rubber used for HV outdoor insulation,” IEEE Transactions on Electrical Insulation, Vol.1, Issue6, Dec1994, pp. 1039-1046.
- [32] Gubanski, S. M, Vlastos, A. E, “Wettability of naturally aged silicon and EPDM composite insulators,” IEEE Transactions on Power Delivery, vol. 5, pp. 1527-1535, July 1990.
- [33] Electro V6.0 users and technical manual, Integrated Engineering Software, Canada

APPENDIX A – DATA SET

In this appendix the various data sets that have been used for developing the regression model and the graphs that were obtained when the assumptions were checked is presented.

a) New silicone rubber

Table 6.1. Original data set considered developing linear regression model between Ln (ESDD) and FOV for new silicone rubber

| S.No | ESDD (mg/cm ²) | Ln (ESDD) | FOV (kV) |
|------|-------------------------------|-----------|-------------|
| 1 | 0.12 | -2.12 | 22.50 |
| 2 | 0.18 | -1.71 | 21.50 |
| 3 | 0.22 | -1.51 | 19.00 |
| 4 | 0.25 | -1.39 | 18.00 |
| 5 | 0.32 | -1.14 | 16.75 |
| 6 | 0.12 | -2.12 | 23.00 |
| 7 | 0.18 | -1.71 | 21.00 |
| 8 | 0.22 | -1.51 | 19.50 |
| 9 | 0.25 | -1.39 | 18.50 |
| 10 | 0.32 | -1.14 | 17.25 |
| 11 | 0.12 | -2.12 | 23.00 |
| 12 | 0.18 | -1.71 | 21.00 |
| 13 | 0.22 | -1.51 | 19.50 |
| 14 | 0.25 | -1.39 | 18.50 |
| 15 | 0.32 | -1.14 | 17.25 |

After the initial analysis in Minitab, as observation corresponding to S. No 2 in Table 6.1 was identified as an unusual observation, statistical analysis was performed with the remaining 14 data points as the removal of unusual observation yielded a much improved model.

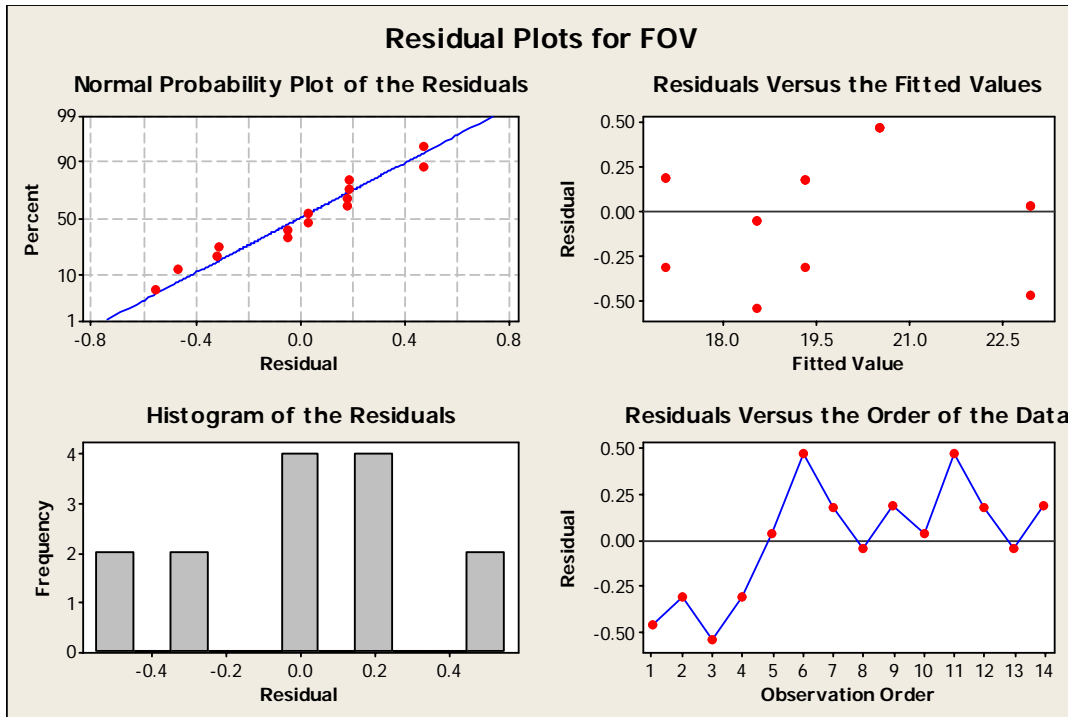


Figure 6.1: Graphs showing various statistical assumptions checked for new silicone rubber model

b) Aged silicone rubber (no recovery)

Table 6.2. Original Data set considered developing linear regression model between Ln(ESDD) and FOV for aged silicone rubber

| S.No | ESDD (mg/cm ²) | Ln (ESDD) | FOV (kV) | S.No | ESDD (mg/cm ²) | Ln (ESDD) | FOV (kV) |
|------|----------------------------|-----------|----------|------|----------------------------|-----------|----------|
| 1 | 0.15 | -1.90 | 19.5 | 16 | 0.32 | -1.14 | 14.5 |
| 2 | 0.156 | -1.86 | 19 | 17 | 0.15 | -1.90 | 20 |
| 3 | 0.17 | -1.77 | 19 | 18 | 0.156 | -1.86 | 19.5 |
| 4 | 0.19 | -1.66 | 18 | 19 | 0.17 | -1.77 | 18.5 |
| 5 | 0.22 | -1.51 | 17.5 | 20 | 0.19 | -1.66 | 18.5 |
| 6 | 0.25 | -1.39 | 16 | 21 | 0.22 | -1.51 | 17 |
| 7 | 0.27 | -1.31 | 16 | 22 | 0.25 | -1.39 | 16.5 |
| 8 | 0.32 | -1.14 | 14.5 | 23 | 0.27 | -1.31 | 16 |
| 9 | 0.15 | -1.90 | 20 | 24 | 0.32 | -1.14 | 15 |
| 10 | 0.156 | -1.86 | 19.5 | | | | |
| 11 | 0.17 | -1.77 | 18.5 | | | | |
| 12 | 0.19 | -1.66 | 18.5 | | | | |
| 13 | 0.22 | -1.51 | 17 | | | | |
| 14 | 0.25 | -1.39 | 16.5 | | | | |
| 15 | 0.27 | -1.31 | 16 | | | | |

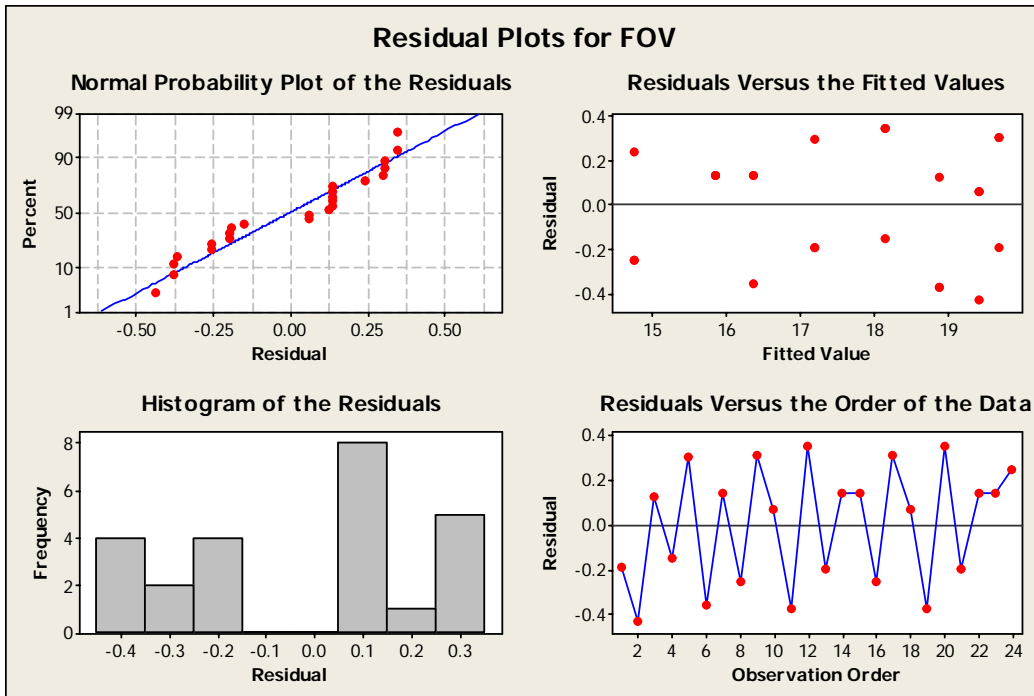


Figure 6.2: Graphs showing various statistical assumptions checked for aged silicone rubber model

c) Aged EPDM

Table 6.3. Original Data set considered developing linear regression model between Ln(ESDD) and FOV for aged EPDM

| S.No | FOV (kV) | ESDD(mg/cm ²) | Ln(ESDD) |
|------|----------|---------------------------|----------|
| 1 | 16 | 0.2 | -1.6094 |
| 2 | 14.5 | 0.23 | -1.46968 |
| 3 | 13 | 0.26 | -1.3471 |
| 4 | 12 | 0.28 | -1.27297 |
| 5 | 10.5 | 0.34 | -1.07881 |
| 6 | 16 | 0.2 | -1.6094 |
| 7 | 15 | 0.23 | -1.46968 |
| 8 | 13 | 0.26 | -1.3471 |
| 9 | 12 | 0.28 | -1.27297 |
| 10 | 10.5 | 0.34 | -1.07881 |
| 11 | 16.5 | 0.2 | -1.6094 |
| 12 | 15 | 0.23 | -1.46968 |
| 13 | 13.5 | 0.26 | -1.3471 |
| 14 | 12.5 | 0.28 | -1.27297 |
| 15 | 11 | 0.34 | -1.07881 |

Initial analysis

Regression Analysis: FOV versus ln(ESDD)

The regression equation is

$$\text{FOV} = -1.14 - 10.7 \ln(\text{ESDD})$$

| Predictor | Coef | SE Coef | T | P |
|-----------|----------|---------|--------|-------|
| Constant | -1.1392 | 0.6816 | -1.67 | 0.119 |
| ln(ESDD) | -10.7253 | 0.4985 | -21.52 | 0.000 |

S = 0.346359 R-Sq = 97.3% R-Sq(adj) = 97.1%

PRESS = 2.07394 R-Sq(pred) = 96.37%

Analysis of Variance

| Source | DF | SS | MS | F | P |
|----------------|----|--------|--------|--------|-------|
| Regression | 1 | 55.540 | 55.540 | 462.97 | 0.000 |
| Residual Error | 13 | 1.560 | 0.120 | | |
| Total | 14 | 57.100 | | | |

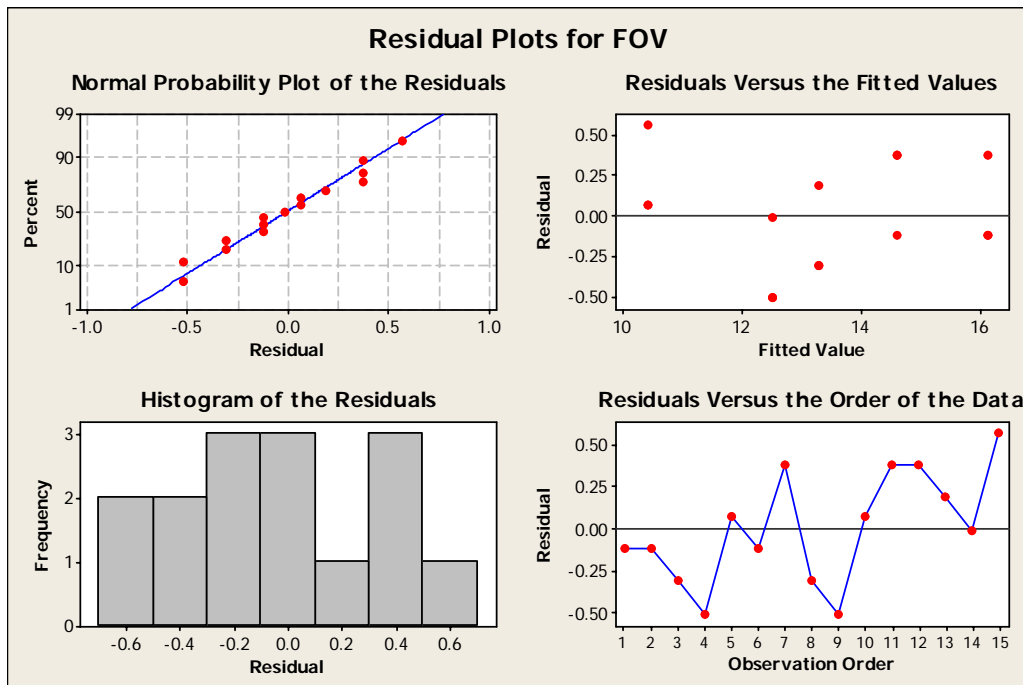


Figure 6.3: Graphs showing various statistical assumptions checked for aged EPDM model (initial analysis)

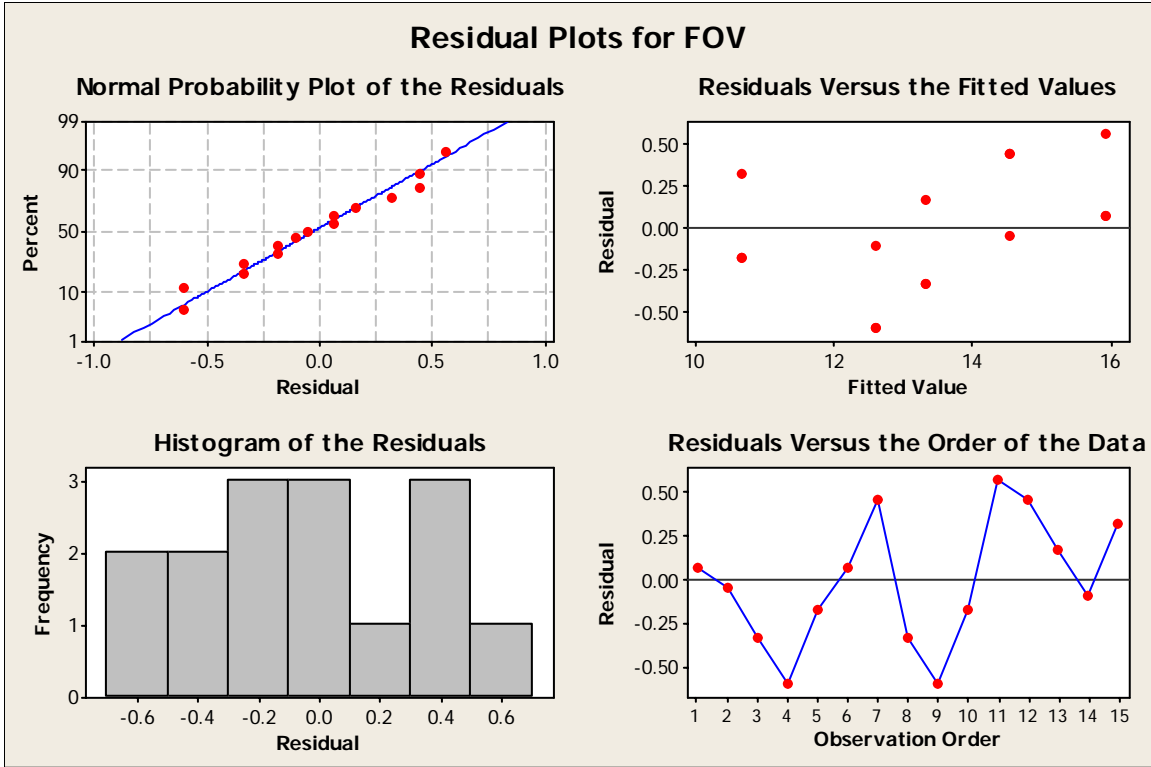


Figure 6.4: Graphs showing various statistical assumptions checked for aged EPDM model (final analysis)

d) Porcelain

Table 6.4. Original Data for developing linear regression model - Ln(ESDD) and FOV of porcelain

| S.No | FOV (kV) | ESDD (mg/cm ²) | Ln(ESDD) |
|------|----------|----------------------------|----------|
| 1 | 16.5 | 0.12 | -2.12026 |
| 2 | 10 | 0.28 | -1.27297 |
| 3 | 8.5 | 0.32 | -1.13943 |
| 4 | 16.5 | 0.12 | -2.12026 |
| 5 | 10 | 0.28 | -1.27297 |
| 6 | 8.5 | 0.32 | -1.13943 |
| 7 | 17 | 0.12 | -2.12026 |
| 8 | 10.5 | 0.28 | -1.27297 |
| 9 | 9 | 0.32 | -1.13943 |

Initial analysis

The regression equation is

$$\text{FOV} = -0.229 - 7.98 \ln(\text{ESDD})$$

| Predictor | Coef | SE Coef | T | P |
|--------------------|---------|---------|--------|-------|
| Constant | -0.2290 | 0.4045 | -0.57 | 0.589 |
| $\ln(\text{ESDD})$ | -7.9836 | 0.2573 | -31.02 | 0.000 |

S = 0.335297 R-Sq = 99.3% R-Sq(adj) = 99.2%
PRESS = 1.26923 R-Sq(pred) = 98.84%

Analysis of Variance

| Source | DF | SS | MS | F | P |
|----------------|----|--------|--------|--------|-------|
| Regression | 1 | 108.21 | 108.21 | 962.54 | 0.000 |
| Residual Error | 7 | 0.79 | 0.11 | | |
| Total | 8 | 109.00 | | | |

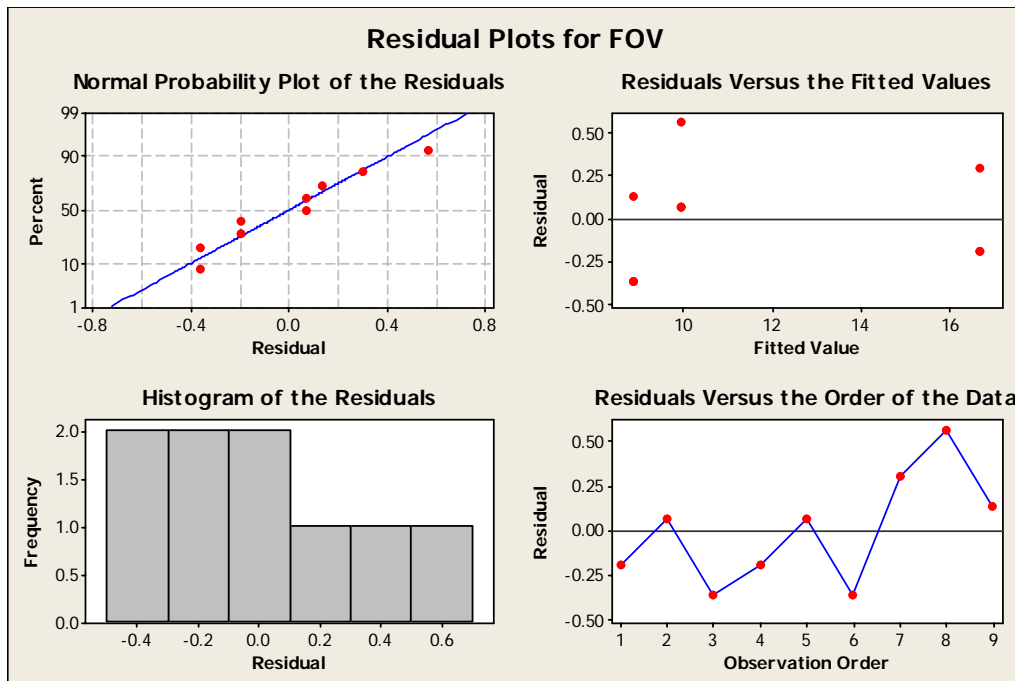


Figure 6.5: Graphs showing various statistical assumptions checked for porcelain (initial analysis)

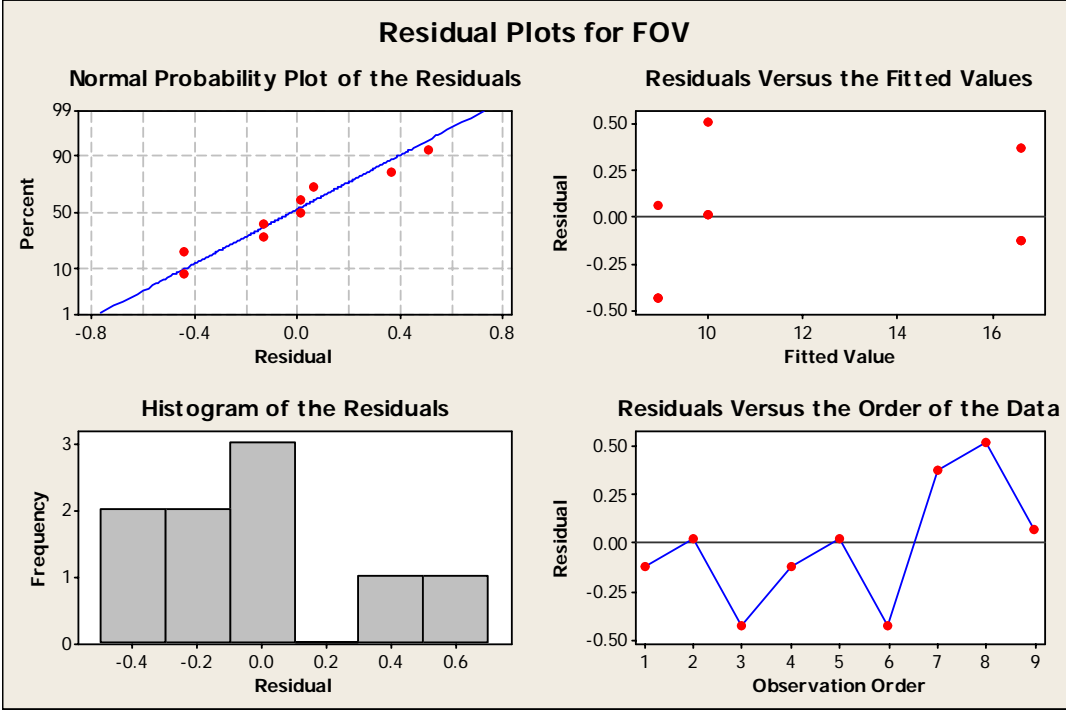


Figure 6.6: Graphs showing various statistical assumptions checked for porcelain (final analysis)

Surface resistance model for aged EPDM

Table 6.5. Values of ESDD, FOV and Surface Resistance for aged silicone and aged EPDM.

| ESDD (SIR) | FOV (SIR) | SR (MΩ/cm) (SIR) | ESDD (EPDM) | FOV (EPDM) | SR (MΩ/cm) (EPDM) |
|------------|-----------|---------------------|----------------|------------|----------------------|
| 0.13 | 20.83 | 1.09 | 0.18 | 16.67 | 0.29 |
| 0.17 | 18.67 | 0.77 | 0.2 | 16.17 | 0.22 |
| 0.19 | 18.33 | 0.65 | 0.26 | 13.17 | 0.15 |
| 0.22 | 17.17 | 0.62 | 0.28 | 12.17 | 0.12 |
| 0.25 | 16.33 | 0.57 | 0.34 | 10.67 | 0.09 |
| 0.27 | 16.00 | 0.47 | | | |

Table 6.6. Original Data set considered developing linear regression model between Ln(Surface resistance) and FOV for aged EPDM

| S.No | Surface resistance (Mohm/cm) | Ln (Surface resistance) | FOV (kV) |
|------|------------------------------------|----------------------------|-------------|
| 1 | 0.22 | -1.51413 | 16 |
| 2 | 0.15 | -1.89712 | 13 |
| 3 | 0.12 | -2.12026 | 12 |
| 4 | 0.22 | -1.51413 | 16 |
| 5 | 0.15 | -1.89712 | 13 |
| 6 | 0.12 | -2.12026 | 12 |
| 7 | 0.22 | -1.51413 | 16.5 |
| 8 | 0.15 | -1.89712 | 13.5 |
| 9 | 0.12 | -2.12026 | 12.5 |

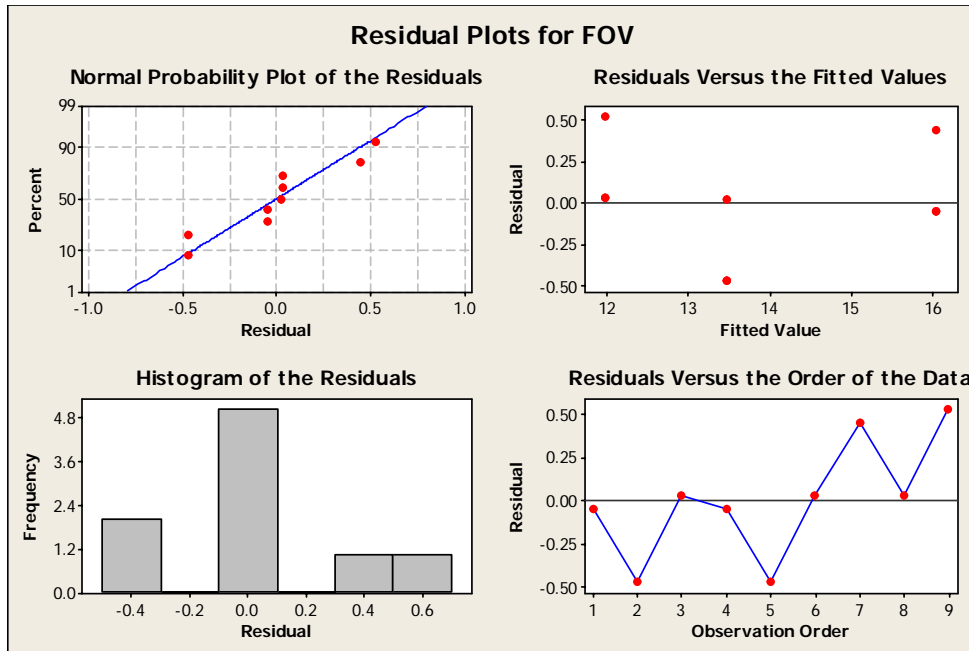


Figure 6.7: Graphs showing various statistical assumptions checked for aged EPDM

Leakage distance based models

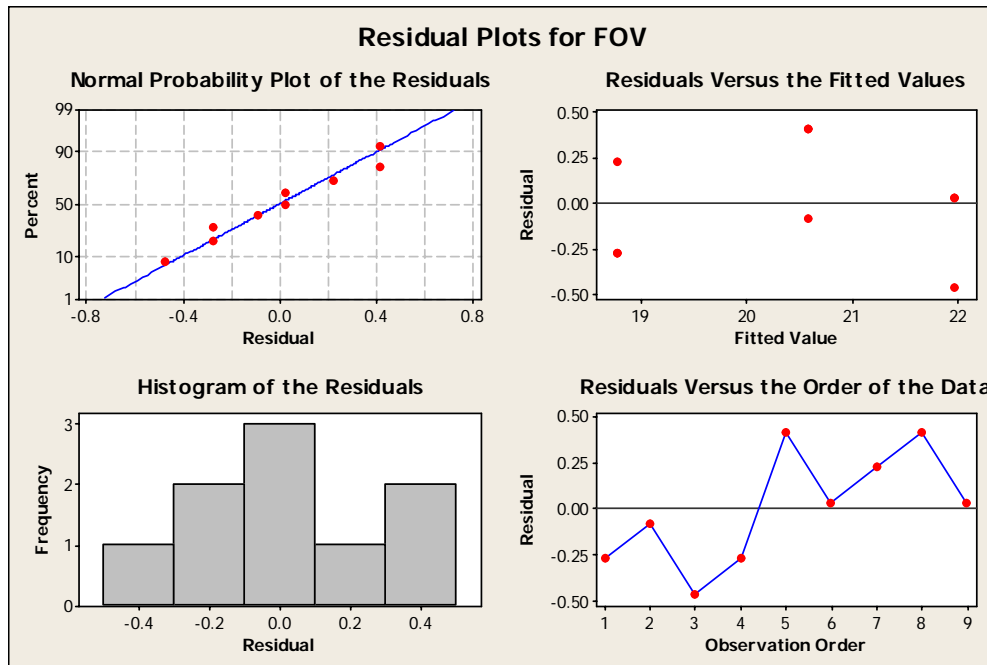


Figure 6.8: Graph showing normality assumption checked for aged EPDM

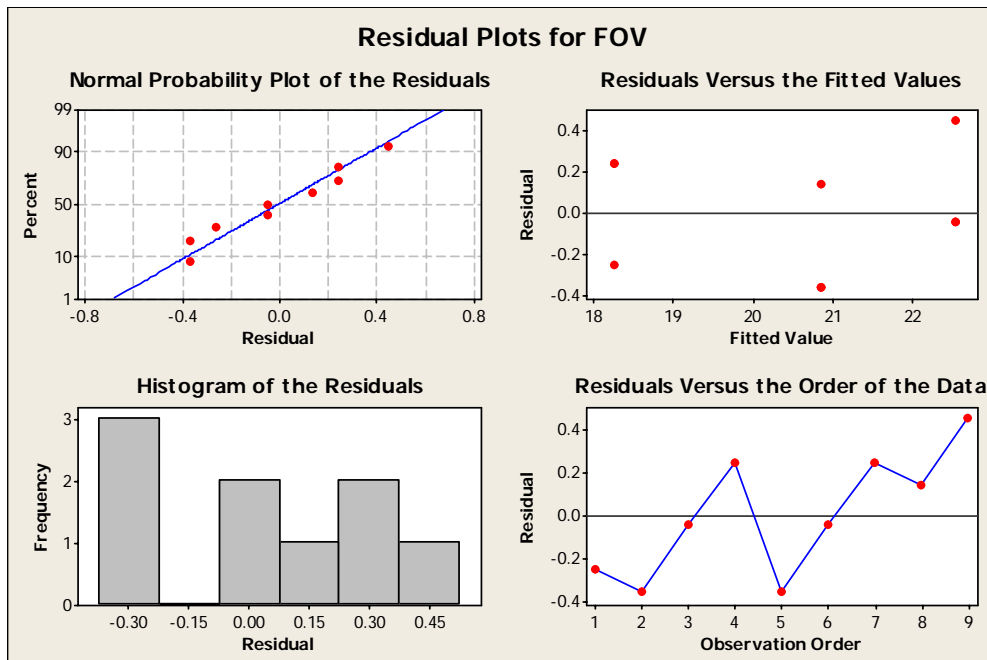


Figure 6.9: Graphs showing various statistical assumptions checked for aged silicone rubber no recovery / New EPDM based on leakage distance

E - Field Analysis

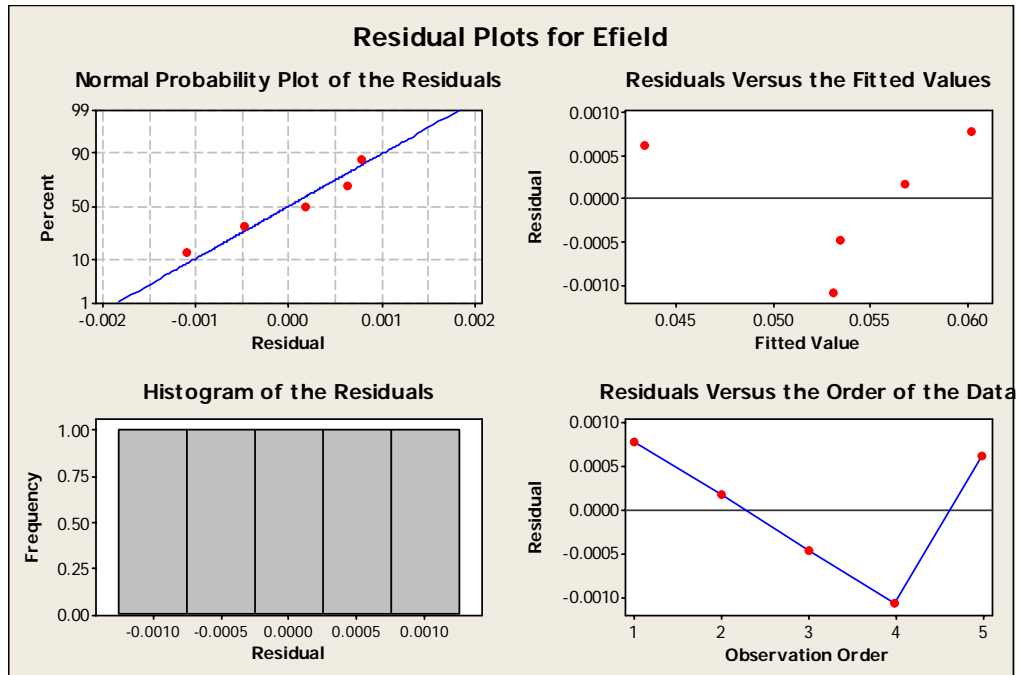


Figure 6.10: Graphs showing various statistical assumptions checked for porcelain model

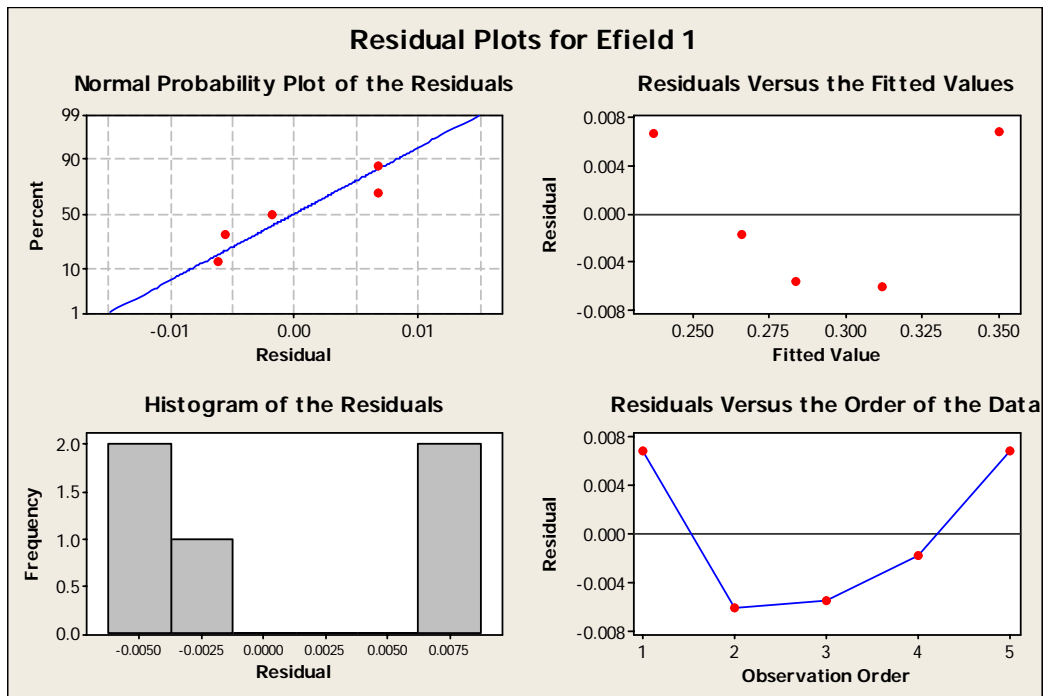


Figure 6.11: Graphs showing various statistical assumptions checked for silicone rubber model

APPENDIX B – PROJECT PUBLICATIONS

Peer reviewed Journals:

- **S.Venkataraman, R. S. Gorur** “Prediction of flashover voltage of non ceramic insulators under contaminated conditions,” IEEE Transactions on DEIS, Vol. 13, Issue 4, pp. 862-869, 2006.
- **S.Venkataraman, R. S. Gorur** “Extending the Applicability of Insulator Flashover Models by Regression Analysis,” Paper Number 1394, Accepted for publication in IEEE Transactions on DEIS, 2006.

Conference Publications:

- **S.Venkataraman and R. S. Gorur**, “Flashover voltage prediction of outdoor insulators subjected to road salt contamination,” Proceedings of the IEEE Conference on Electrical Insulation and Dielectric Phenomena, 293 – 296, 2005.
- **S.Venkataraman and R. S. Gorur**, “A novel method for prediction of flashover of in-service EPDM insulators,” Proceedings of the IEEE Conference on Electrical Insulation and Dielectric Phenomena, pp, 385-388, 2006.
- **S.Venkataraman and R. S. Gorur**, “Non Linear Regression Model to Predict Flashover of Non-ceramic Insulators ,” Proceedings of IEEE North American Power Symposium, pp. 815-818, 2006.